

UNIVERSITÀ DEGLI STUDI DI PADOVA

Facoltà di Ingegneria

Corso di Laurea Magistrale in Ingegneria Elettrica

**Accurate evaluation of the ground impedance  
of real earthing systems**

Relatore: **PROF. ROBERTO TURRI**

Dipartimento di Ingegneria Elettrica

Laureando : **Leggio Massimiliano**

Anno Accademico 2011/2012



## Table of contents

Sommario .....	5
Introduction .....	11
1 Earth resistivity .....	13
1.1 Introduction.....	13
1.2 Effect moisture, temperature, salt .....	13
1.3 Effect of voltage gradient and current magnitude.....	14
1.4 Resistivity measurements.....	15
1.4.1 Introduction.....	15
1.4.2 Wenner four-point method.....	16
1.4.3 Unequally-spaced or Schlumberger-Palmer Arrangement.....	18
1.5 Interpretation of soil resistivity measurements .....	19
2. Measurements of earth impedance for grounding system.....	21
2.1 Introduction.....	21
2.2 Fall of potential Method.....	21
2.3 Measurement error for the Fall-of Potential method.....	25
2.3.1 Measurement Error Due to Earth Mutual Resistances .....	25
2.3.2 Measurement Error due to AC Mutual Coupling.....	26
2.3.3 Mutual Coupling to Potential Lead Extend Ground Conductors .....	27
2.4 Practical testing considerations .....	27
2.5 Behaviour of earthing system under high frequency .....	29
3. Measurements Using the Fall-of –Potential Method.....	31
3.1 Uniform Soil .....	31
3.2 Different Lead Separation Distances .....	32
3.3 Low Resistivity Uniform Soils.....	32
3.4 High Operating Frequencies .....	33
3.5 Small Grounding Grid.....	34
3. 6 Conclusions.....	35
4 Carson-Clem method and Complex-image method .....	37
4.1 Introduction.....	37
4.2 Carson’s formula.....	37
4.3. Carson-Clem formula.....	39

4.4 Expression to evaluate the mutual coupling between parallel or angled conductors of finite length.....	39
4.5 Comparison between Complex-image method and Carson-Clem method .....	41
4.6 Conclusions.....	46
5 Field Tests by using the Fall Of Potential method.....	47
5.1 Introduction.....	47
5.2 Characteristics grid and soil.....	47
5.3 Test 1 : Fall of potential Method with angled leads.....	50
5.4 Test 2 : Fall of potential Method with parallel leads, separation 1 m.....	52
5.5 Test 3 : Fall of potential Method with parallel leads, separation about 0,06 m.....	57
5.6 Conclusions.....	62
6.1 Introduction.....	63
6.2 Laboratory.....	64
6.3 Field tests.....	68
6.4 Conclusions.....	71
7 General Conclusions .....	73
Acknowledgements.....	75
Appendix A.....	77
Appendix B.....	81
References.....	83

## Sommario

A conclusione del percorso di studi universitari mi è stata offerta la possibilità, grazie al programma Erasmus Placement e al Prof. Roberto Turri, di passare un periodo di circa quattro mesi presso l'Università di Cardiff (UK). L'obiettivo di questa esperienza è stato quello di svolgere il tirocinio universitario necessario per la preparazione della tesi di laurea magistrale, nonché quello di arricchire la conoscenza della lingua inglese e crescere a livello personale dovendomi trovare in un ambiente totalmente estraneo, con le varie difficoltà che ne derivano. Il tirocinio si è svolto presso il Dipartimento di Ingegneria Elettrica dell'Università di Cardiff, associato al gruppo di ricerca HIVES (High Voltage Energy Research Group). L'obiettivo del lavoro è stato principalmente quello di cercare di ricavare il valore della resistenza di terra di una griglia di dimensioni 3 x 3 m collocata a Llanrumeny Cardiff (Regno Unito).

Il tirocinio si può suddividere in tre fasi principali:

- i) La prima è stata concentrata ad acquisire tutte le necessarie conoscenze che riguardano gli impianti di terra e i parametri d'influenza.
- ii) La seconda parte è stata caratterizzata da una fase di analisi numerica con l'utilizzo del software CDEGS per la valutazione dell'impedenza di terra della griglia ed una breve fase in cui ho avuto l'occasione di lavorare in laboratorio su un nuovo metodo per il calcolo dell'impedenza di terra con cavo coassiale. Ho potuto quindi familiarizzare con diverse attrezzature che poi sarebbero state utilizzate nella fase successiva.
- iii) L'ultimo periodo infatti l'ho passato ad effettuare delle misure sul campo da confrontare con le simulazioni. In questo stesso lasso di tempo con i dati ho iniziato la stesura della tesi.

La misura della resistenza di un sistema di terra è stato un argomento ampiamente studiato e vastamente descritto in letteratura per via della sua grande importanza per quel che concerne il mantenimento dei limiti di sovratensioni conseguenti a guasti o fulminazione e perciò per garantire la sicurezza delle apparecchiature, ma soprattutto delle persone. Dato il ruolo fondamentale che svolge nella definizione della resistenza di terra, diversi studi sono stati concentrati ad uno dei fattori più importanti che ne definiscono il valore, la resistività del terreno. La misura della resistività del terreno è essenziale per la stesura di un progetto perché, nonostante i risultati siano incerti e variabili, ci permettono di calcolare in prima approssimazione il valore che dovrebbe avere il sistema di terra. Le tecniche per misurare la resistività del terreno sono essenzialmente le stesse qualsiasi sia lo scopo della misura. Grande importanza sono i vari i parametri d'influenza come la variazione del contenuto dei umidità, la temperatura o compattezza del suolo. Evidente è perciò la mutevolezza della resistenza a causa delle variazioni stagionali. Un'altra difficoltà è rappresentata interpretazione dei dati raccolti può variare considerevolmente, specialmente quando si ha a che fare con terreno non uniformi. La complessità causata da terreni non uniformi è

molto comune e solo in pochi casi la resistività del terreno è costante all'aumentare della profondità. Di solito ci sono diversi strati ognuno con differenti resistività, mentre variazioni laterali possono verificarsi ma di solito sono graduali e trascurabili nelle vicinanze del sito considerato. Inoltre, essendo il sistema di terra chiamato a disperdere correnti di guasto e correnti conseguenti a fulminazione ed essendo sottoposto a tutte le correnti di dispersione circolanti nel terreno, ulteriori variazioni del valore della resistenza possono avvenire nel corso degli anni a causa della deterioramento del sistema stesso. Da quanto detto appare evidente la necessità di periodiche misurazioni della resistenza di terra per accertarsi che non si siano superati i limiti di sicurezza o comunque per acquisire tutte quelle informazioni necessarie per la progettazione di successivi e più efficienti sistemi di terra.

Il fall of potential method è uno dei metodi maggiormente usati per valutare la resistenza di terra. Il suo valore è dato da una misura volt-amperometrica ma che può essere soggetta a diverse cause d'errore, una delle quali è il flusso concatenato tra i due conduttori. Per valorizzare il mutuo accoppiamento, una delle vie può essere analitica. In letteratura sono stati sviluppati differenti metodi analitici aventi caratteristiche differenti. Un confronto tra la formula semplificata di Carson-Clem utilizzabile solo per conduttori paralleli e un altro metodo, che per comodità chiamo Image formula, che permette di valutare il mutuo accoppiamento anche per conduttori non solamente paralleli. Il confronto è stato effettuato in funzione di diversi parametri: la resistività del terreno, la distanza tra i conduttori, la loro lunghezza e la frequenza. L'errore relativo è stato perciò valutato considerando come standard i valori ottenuti tramite la formula semplificata di Carson-Clem, tenendo in considerazione che quest'ultima è affetta da errore massimo del 2.5 % rimanendo all'interno di alcuni limiti. Ho potuto notare un considerevole errore relativo, anche del 40 % per conduttori di breve lunghezza, con una sottostima della componente reattiva del mutuo accoppiamento da parte di Image formula.

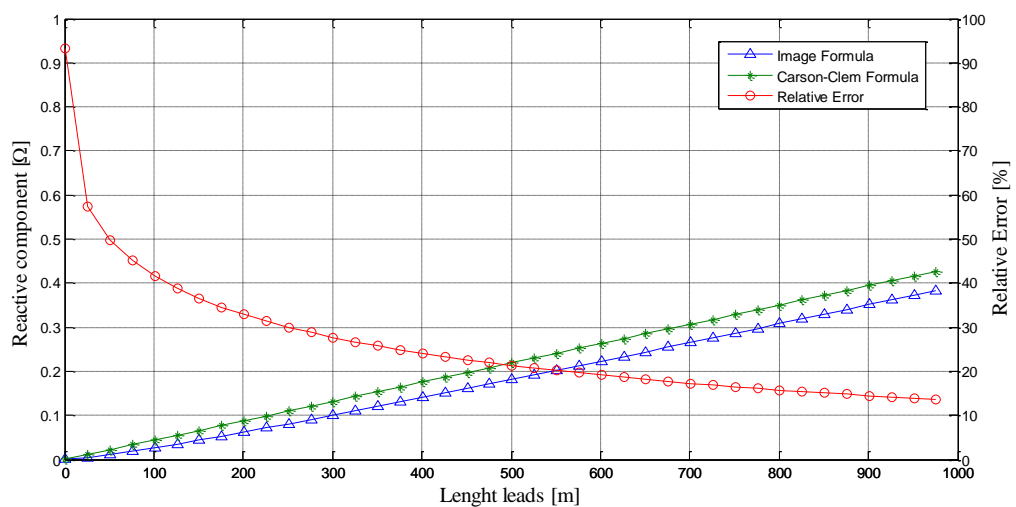


Figura 1 Componente reattiva calcolata con Carson-Clem e Image Formula

Come detto ruolo fondamentale svolge la resistività del terreno sul valore dell'impedenza di terra. Per scegliere il modello che rappresenti il comportamento del terreno mi sono fornito di alcune misurazioni effettuate in diversi anni precedenti e rappresentati nella seguente figura.

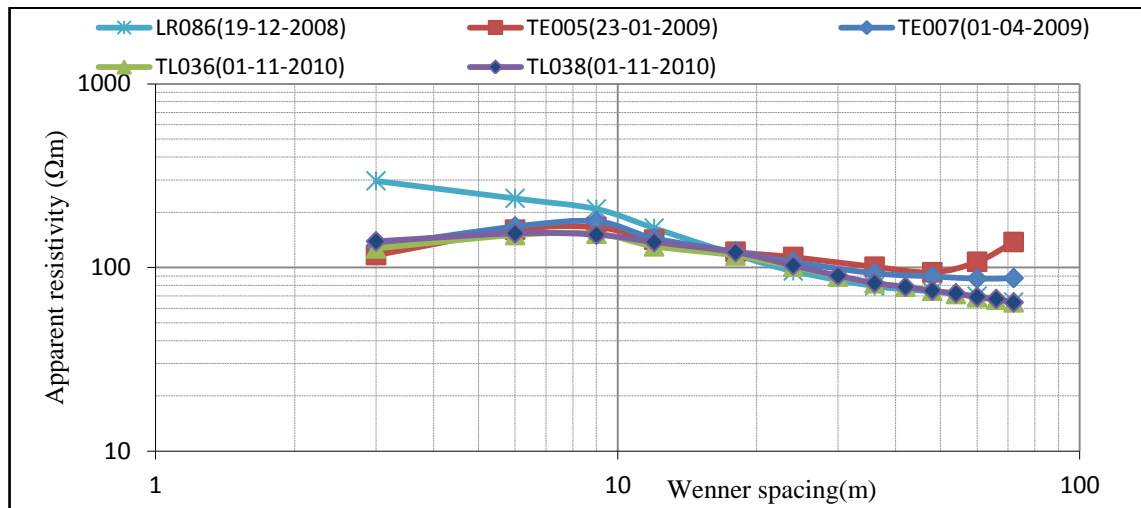


Figure 2 Resistività del terreno.

Visto gli andamenti e i valori della resistività del terreno considerati, ho deciso di utilizzare un modello a due strati con lo strato superiore di resistività  $150 \Omega\text{m}$  e profondità  $7 \text{ m}$  mentre per lo strato inferiore una resistività di  $70 \Omega\text{m}$  ed una profondità infinita. La griglia analizzata di dimensioni  $3 \times 3 \text{ m}$  si trova a mezzo metro sotto il livello del suolo, quindi si tratta di un piccolo impianto di terra di elevata impedenza, confermato in prima analisi da un valore di  $21.56 \Omega$  calcolato tramite la formulazione adattata per terreni a due strati. La parte analisi numerica con il software CDEGS della resistenza di terra è stata valuta in funzione della frequenza per tre tipi di set-up:

- i) Cavi perpendicolari
- ii) Cavi ad una distanza di  $1 \text{ m}$
- iii) Cavi ad una distanza di  $0.06 \text{ m}$

Queste simulazioni sono state poi replicate e confrontate nelle misurazioni.

Nella figura seguente rappresenta il set-up per cavi ad una distanza di 1 m ed un'analisi che va dai 52 Hz fino ai 70 kHz. La resistenza di terra al variare della frequenza presenta dei trend simili tra simulazione e le misurazioni.

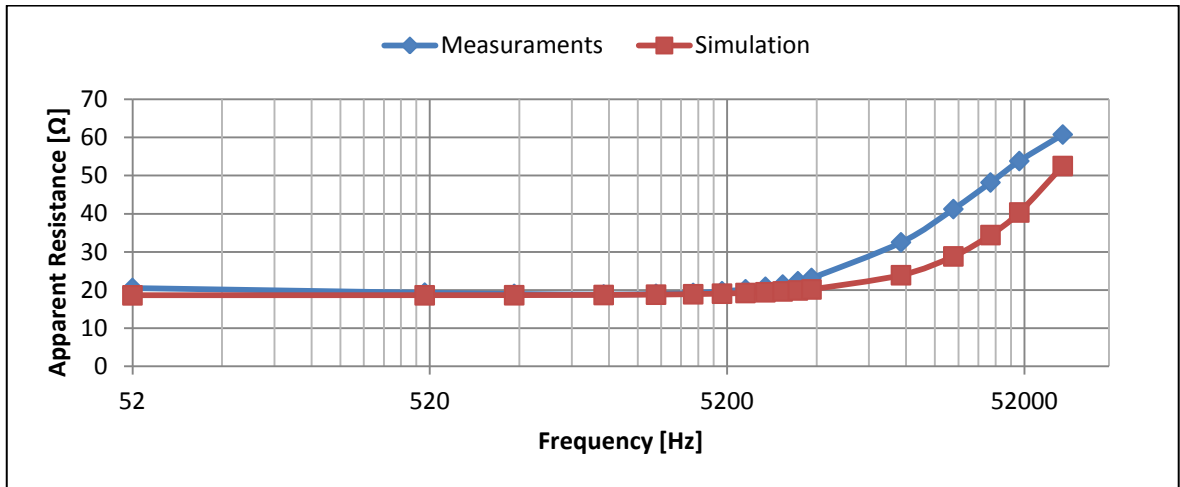


Figura 3 Impedenza di terra calcolata attraverso le misure e la simulazione

Alcune differenze si presentano tra le due analisi con errori relativi, prendendo le misurazioni come standard, massimi del 10 %. Una delle ragioni di questa differenza è dovuta probabilmente alla scelta del modello del terreno che non rappresenta il reale comportamento. Questo conferma come costanti misurazioni sono necessarie per la valutazione dell'impedenza di terra anche se la continua urbanizzazione complica questa necessità. Un ulteriore confronto dai dati raccolti è stato fatto per il calcolo della mutua impedenza ottenuta tramite la formula Image e le misure, per frequenze da 52 Hz ai 10 kHz . Per mutua impedenza ottenuta tramite le misure si intende la differenza tra il valore della resistenza di terra con conduttori paralleli meno sempre il valore ottenuto della resistenza di terra ma con conduttori perpendicolari. Dalla figura seguente esiste una buona corrispondenza tra i due metodi con conduttori ad una distanza 1 m mentre per una separazione di 6 cm ciò non avviene. Ulteriori misurazioni dovrebbero essere effettuate per confermare le misure effettuate e cercare se capire se esiste una distanza oltre la quale la formula analitica non è applicabile.

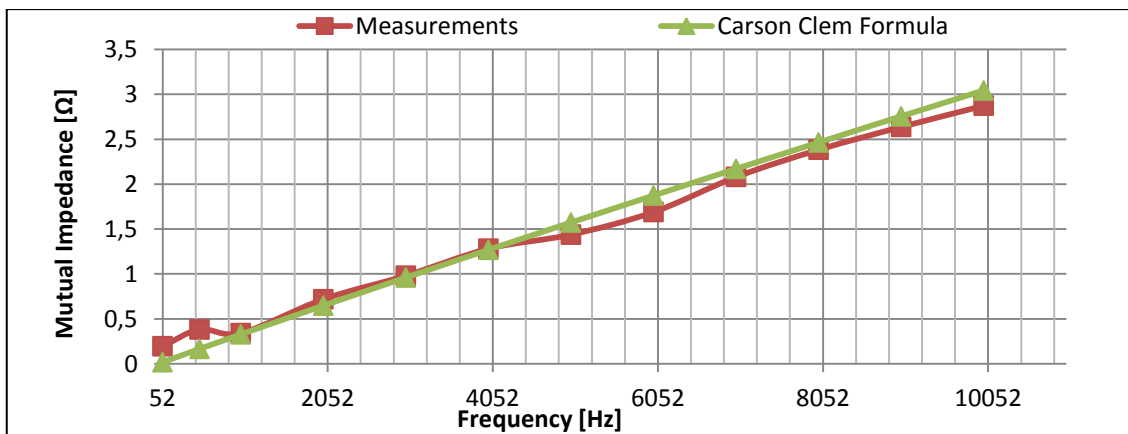
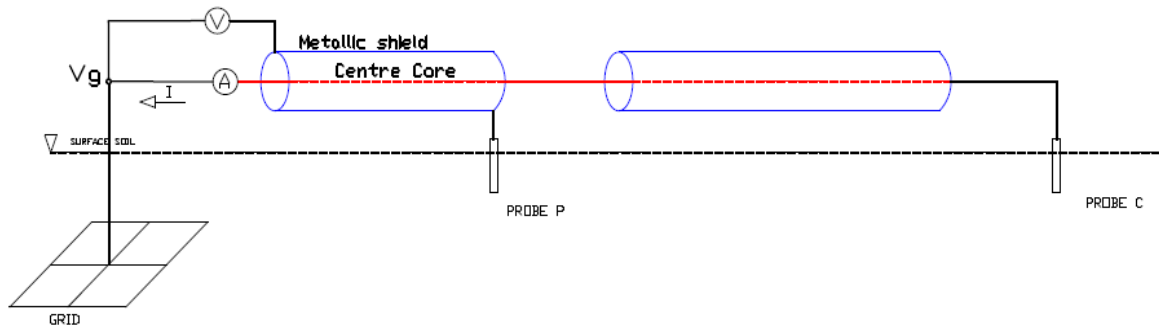


Figura 4-a 4-b Mutua Impedenza con separazione di 1 m e 6 cm



Un nuovo metodo per la valutazione della resistenza di terra è stato idealizzato come mostra la figura 5. Si tratta sempre di una misura volt-amperometrica, dove però a differenza del Fall of Potential Method si utilizza un unico cavo coassiale. La corrente viene fatta scorrere tra il sistema di terra e la sonda C tramite il nucleo del cavo mentre la tensione viene misurata attraverso lo schermo.



*Figura 5 Fall of potential con cavo coassiale*

Pure questo metodo può comportare degli errori di valutazione dell'impedenza di terra a causa del mutuo accoppiamento tra nucleo e schermo. Una breve analisi sia in laboratorio che con delle misure sul campo è stata effettuata per capire quale fosse la fattibilità del metodo ed effettuare alcune valorizzazioni del mutuo accoppiamento.

Nei test sul campo solo alcune frequenze sono state analizzate, quindi un confronto con il Fall of Potential Method non pienamente auspicabile. Tuttavia alcune considerazioni possono essere tratte. La resistenza di terra della griglia alla frequenza di 52 Hz è molto simile a quella ottenuta con conduttori perpendicolari, questo grazie ad una bassa frequenza ed ad una lunghezza del conduttore coassiale relativamente corta da non creare un importante mutuo accoppiamento, dimostrando così una possibile applicabilità del metodo per impianti di terra di piccole dimensioni. Per frequenze di 500 Hz e 20 kHz il mutuo accoppiamento risulta sicuramente maggiore rispetto agli altri test, grazie ad una maggiore vicinanza tra nucleo e schermo. Il calcolo del mutuo accoppiamento viene effettuata con l'utilizzo della formula di Carson-Clem riadattata per cavi coassiali. È stato rilevata non un ottima precisione nella valorizzazione di questo fenomeno se messo a confronto con il test effettuato con conduttori perpendicolare. Ragioni possono essere dovute alla non applicabilità di Carson-Clem per terreni uniformi. Per ottenere una più accurata valutazione dell'applicabilità di questo metodo e le problematiche che ne derivano ulteriori test dovrebbero essere effettuati, soprattutto sistemi di terra di dimensioni più ampie, per capirne la validità.



## Introduction

*In principle, a safe grounding system has the following two objectives:*

- To provide means to carry electric currents into the earth under normal and fault conditions without exceeding any operating and equipment limits or adversely affecting continuity of service.*
- To assure that a person in the vicinity of grounded facilities is not exposed to the danger of critical electric shock.*

*Measurements of ground resistance or impedance are necessary to verify the adequacy of a new grounding systems, this thesis reviews the main method of measurement, the Fall-of Potential Method, for the evaluation of the ground impedance for grounding systems and the various factors of influence. The ground impedance was assessed for a small grid by a comparison between measurements and numerical analysis, simulations.*

*This project was developed during the ERASMUS PLACEMENT program done in the High Voltage Energy Systems Research Group of the School of Engineering of Cardiff University, United Kingdom under the supervision of Professor Huw Griffiths .*



# **1 Earth resistivity**

## **1.1 Introduction**

The measurement of soil resistivity is prior to the drafting of the project because, despite the measurement results are rather uncertain and variable, allows us to calculate a first approximation the value that should take the grounding system.

The techniques for measuring the soil resistivity are essentially the same whatever the purposes of measurement . However, the interpretation of the recorded data can vary considerably, especially where soils with non-uniform resistivity is encountered. The added complexity caused by non-uniform soils is common, and in only few cases are the soil resistivity is constant with increasing depth. Usually there are several layer, each having a different resistivity. Lateral changes may also occur, but in general these changes are gradual and negligible at least in the vicinity of the site concerned. [2] This variability makes the construction of the earth models for the design of grounding system a very difficult task.

## **1.2 Effect moisture, temperature, salt**

Electrical conduction in soil is essentially electrolytic. For this reason the resistivity of most soils rises abruptly whenever the moisture content accounts for less than 15% of the soil weight. The amount of moisture further depends upon the grain size, compactness, and variability of the grain sizes. However, as shown in curve 2 of figure 6, the resistivity is little affected once the moisture content exceeds approximately 22%. The effect of temperature on soil resistivity is nearly negligible for temperatures above the freezing point. At 0°C, the water in the soil starts to freeze and resistivity increases rapidly. Curve 3 shows this typical variation for a sandy loam soil containing 15.2% of moisture by weight. The composition and the amount of soluble salts, acids, or alkali present in the soil may considerably affect its resistivity. Curve 1 illustrates a typical effect of salt (sodium chloride) on the resistivity of a containing 30% moisture by weight [1]. In frozen soil, as in the surface layer in winter the resistivity may be exceptionally high [2].

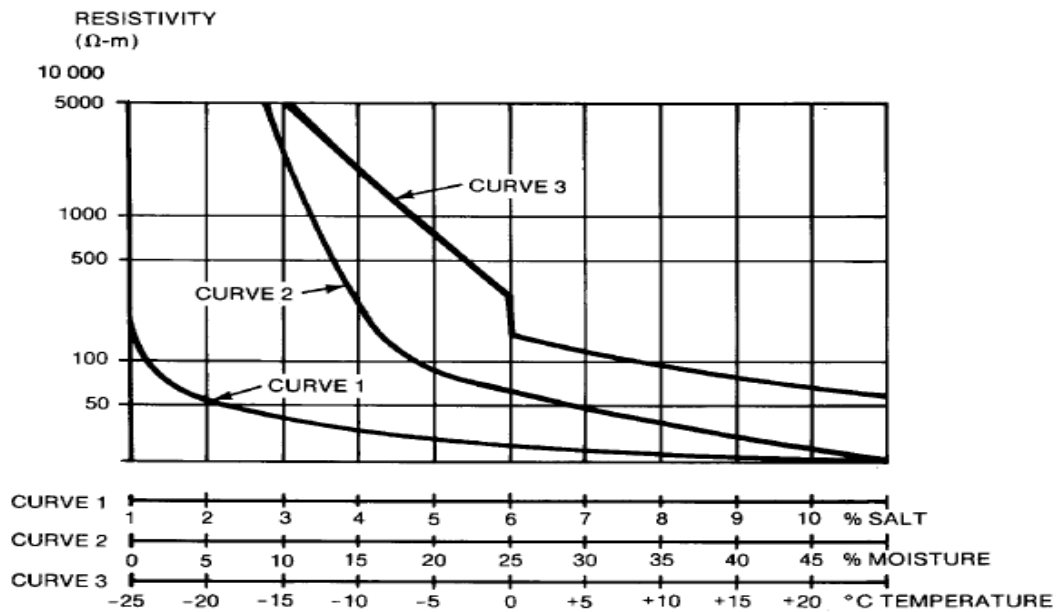


Figure 6 Effects of salt, moisture, temperature upon soil resistivity  
(Reproduced from [1])

### 1.3 Effect of voltage gradient and current magnitude

The soil resistivity is not affected by a voltage gradient unless it exceeds certain values. The value changes in some way with the kind of soil material, but usually it has a value of several KV/cm. Because the substation grounding system normally is designed to comply with far more stringent criteria of step and touch limits, the gradient can always be assumed to be below the critical range.

Regarding the current the soil resistivity may be affected by it flowing from the electrodes into the surrounding soil. The thermal characteristic and the moisture content of the soil will determine if a current is able to make a significant drying and thus increase the effective soil resistivity. A conservative value of current density has not to exceed 200 A/m<sup>2</sup> [1].

As shown in figure 7 the range of resistivity for different soil and rock is pretty wide. It can vary from values of 10 Ω·m (clays) to 10<sup>6</sup> Ω·m (granities), considering that the resistivity increases with the age of the geological formation.

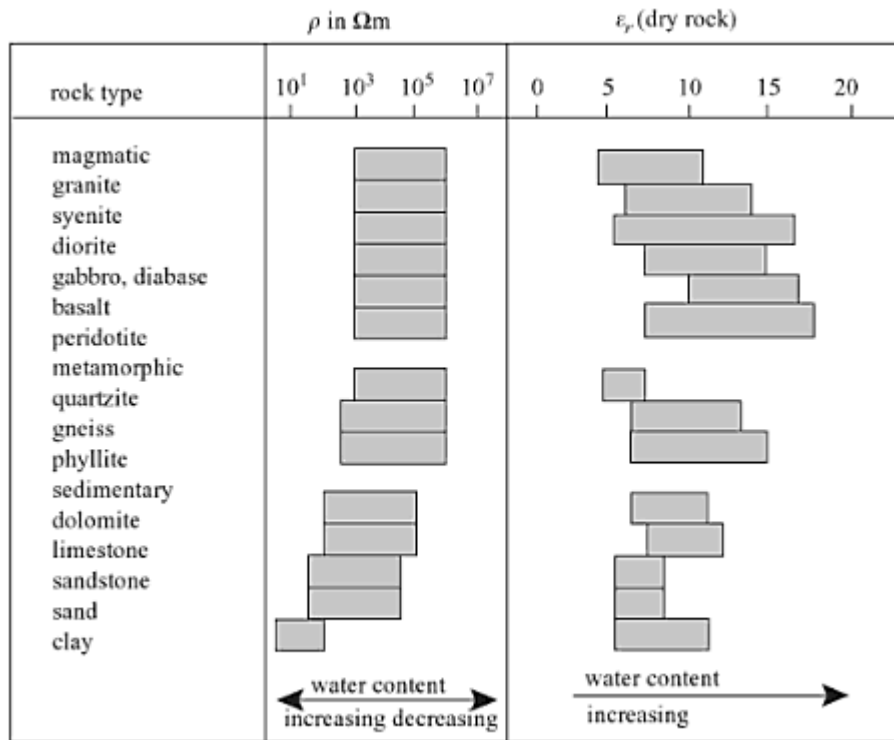


Figure 7 Mean value ranges of resistivity and permittivity for different rock types  
( Reproduced from [5] )

This table makes it clear how can be difficult estimate the earth resistivity from a geological classification; season variations in the water content and temperature variations at the soil surface may also have an effect. For these reasons and those previous explained only through specific measurements on the field to investigate is possible have reasonable and realistic values of earth resistivity [5].

## 1.4 Resistivity measurements

### 1.4.1 Introduction

A wide knowledge of the soil resistivity is the first and important step to define a safety grounding system. Vary tools can be useful, like geological maps, borehole data, seismic surveying and ground penetrating radar, these are helpful for identifying physical boundaries in the earth and have an idea of resistivity range. However these tools are insufficient as are in same way measurements by itself, conjunction with one or more methods for identifying earth region boundaries with measurements on the site investigation may offer an earth model of most merit.

The most accurate method in practice of measuring the resistivity of large volumes is the four-point method. There are two variations of four-point method often used, one the Wenner four-point method and another one is Unequally-spaced or Schlumberger-Palmer Arrangement.

It is necessary taking into account during earth resistivity measurements the proximity of buried extending earth grid or the routes of the substation's underground cable circuits. The presence of metallic object provides an underestimation of the earth resistivity that is not in every case so clear to identify and confusable with the natural heterogeneity of the earth (see item 2.3).

### 1.4.2 Wenner four-point method

Four probes are driven into the earth along a straight line, at equal distances  $a$  apart, driven to a depth  $b$ . The voltage between the two inner (potential) electrodes is then measured and divided by the current between the two outer (current) electrodes to give a value of resistance  $R$ .

The figure 8 shows the Wenner Method made up of four probes at equal distances.

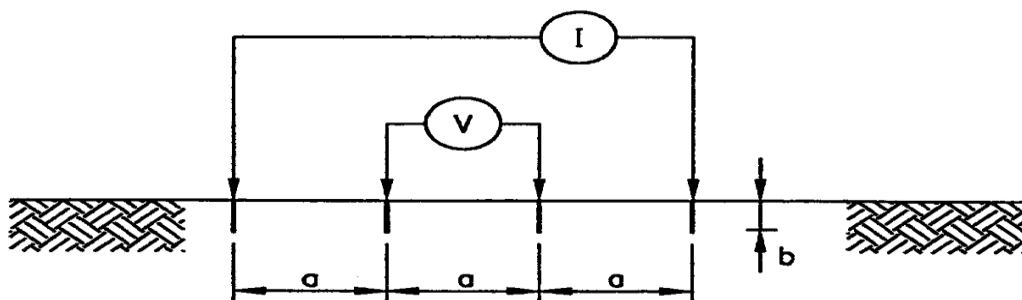


Figure 8 The Wenner Method  
( Reproduced from [2] )

From the ratio between the voltage and current measured is possible to obtain apparent resistivity  $\rho_a$  in terms of the length units, it related to  $R$  by the formula 1 :

$$\rho_a = \frac{4\pi a R}{1 + \frac{2a}{\sqrt{a^2 + 4b^2}} - \frac{a}{\sqrt{a^2 + b^2}}} \quad [\Omega \cdot m] \quad (1)$$



where :

a= distance between two adjacent electrodes

b = buried depth electrodes.

The electrodes typically are placed in the straight line and to a depth not more of 0.1 a. If b is small compared to a, as is the case of probes penetrating the ground only a short distance, the equation gets:

$$\rho = 2\pi aR \quad [\Omega \cdot m] \quad (2)$$

The current tend to flow near the surface when the probe spacing is relatively small, while the current flow deeper for bigger probe spacing. Thus, it is usually a reasonable approximation to assume that the resistivity measured for a given probe spacing a represents the apparent resistivity of the soil to a depth of a, as shown in figure 9 where the resistivity is given for different spacing probes. This rule should be used with caution, because the correspondence between spacing and depth is only an approximation .

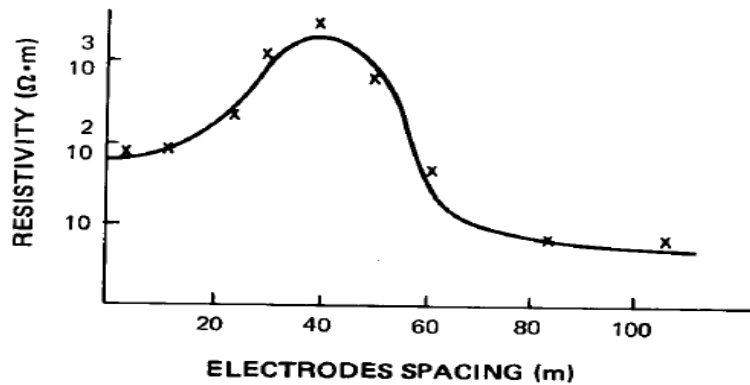


Figure 9 Apparent resistivity curve ( Reproduced from [2] )

As mentioned in 1.1 the lateral changes of earth resistivity are more usual than vertical changes, resistivity changes considerably with the depth is necessary increase the spacing electrode for analyzing deeper layer.

### 1.4.3 Unequally-spaced or Schlumberger-Palmer Arrangement

This set up respect the Wenner brings with it a small different, the potential probes are brought nearer the current probes, as shown in figure 10 this for solving the shortcoming Wenner Method has, in fact it is unsuitable when the distance between the electrodes increase considerably, the magnitude of potential between the inner electrodes can decrease so that commercial instruments are inadequate for measuring such low potential and a high value of current magnitude is not usually available.

If the depth of burial of electrodes  $b$  is small compared to their separation  $d$  and  $c$ , then the measured resistivity can be calculated as :

$$\rho = \frac{\pi c(c + d)R}{d} \quad [\Omega \cdot m] \quad (3)$$

where:

$d$ =distance between the potential electrodes

$c$ =distance between current electrode and potential electrode

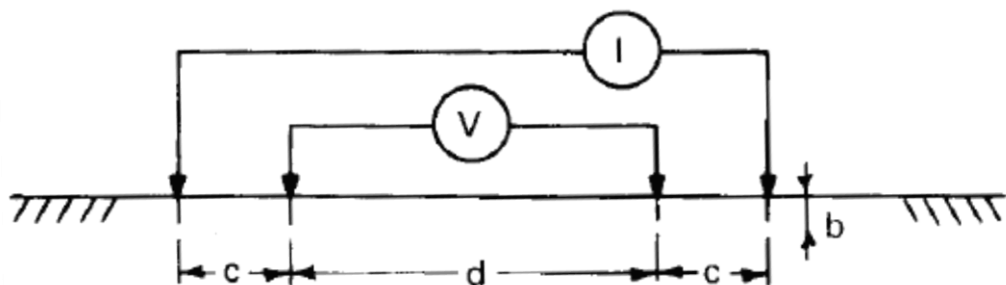


Figure 10 Schlumberger-Palmer method  
( Reproduced from [2] )

Wenner four-point and Schlumberger-Palmer methods are the most popular for different reasons. With it is possible survey deeper layers without driving of the electrodes until these layers, the data are not affected by resistance of the electrodes or holes created in driving electrodes into the soil. Another method “ driven-rod method” , like the four-point method as well, it can provide information useful for the development of a model, but researching at deep layers are not possible.

## 1.5 Interpretation of soil resistivity measurements

The interpretation of soil resistivity measurements is the part most difficult of the measurement program. The choice of which model can represent with more approximation the actual soil is not an easy work. The reasons of this hard task are caused by soils where the resistivity can vary significantly with the depth, depending on soil stratification, and seasonal variations. So the possibility that the soil model perfectly matches the actual condition of the soil is pretty unlikely.

A uniform soil model should be used only when there is a moderate variation in apparent resistivity, which rarely occurs in practice and brings about an approximation that unlikely matches the actual soil. However, this model is convenient because many analytical formulas to calculate the earth resistance for example are based on homogeneous earth assumptions. Another model is a two-layer model, it consists of an upper layer of finite depth and a layer lower with different resistivity and infinite thickness. It can be a model more accurate than a uniform model. In other cases the variation in soil resistivity can be such that even a two-layer model is not adequate, especially when the difference between the maximum and minimum value is large, a multilayer model is so more useful.

The value for a uniform soil resistivity can be found through an average of the measurements made at different spacings in the Wenner-method while for the two-layer model there are several techniques to determine it, in some instances can be approximated by visual inspection of a plot of apparent resistivity versus probe spacing from Wenner measurements.

The figure 11 shows the measurements that have been carried out in different sites of the apparent resistivity plotted against the interelectrode spacing.

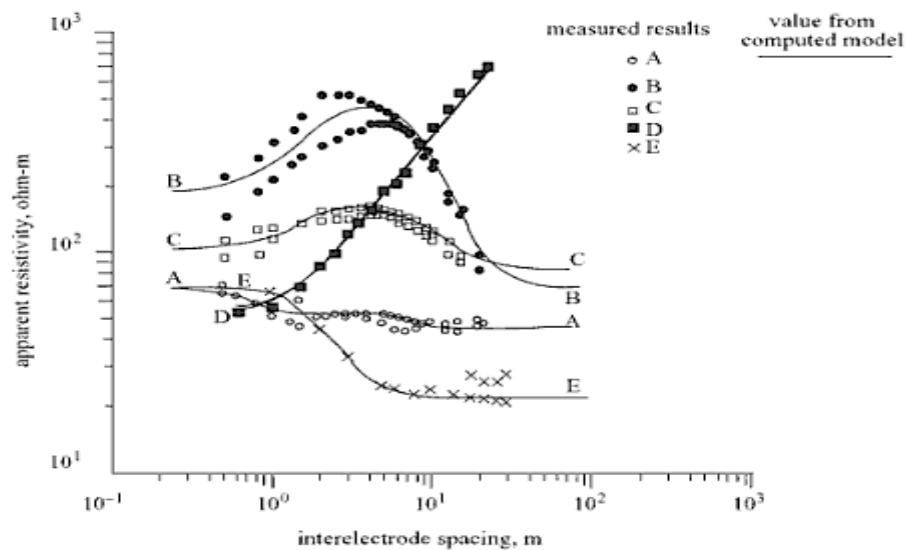


Figure 11 Apparent resistivity versus interelectrode spacing  
( Reproduced from [2] )

For the curve A the apparent resistivity does not change widely with the spacing, for this reason probably it represents a homogeneous earth. The curves E and D changes the own values to represent a non-uniformities in the earth, and a two-layer model can be used, instead the curves B and C the three-layer model. Others model for the interpretation of the earth resistivity are applicable ad the 2-D and 3-D model.

## 2. Measurements of earth impedance for grounding system

### 2.1 Introduction

The best assurance for the effectiveness of a grounding system may be verified by periodically measuring its ground resistance. There are several methods for measuring resistance of a ground electrode system. Among them, as verified in many field tests, the fall-of-potential method is widely applied for almost all types grounding systems and the staged fault test or out-of-service circuit test, these last two are seldom performed due to economic penalties [5]

In this section the ohmic value is called “resistance”, it should be remembered that there is a reactive component that should be taken into account when the ohmic value of the ground under test is less than  $0.5 \Omega$ , and the ground is of relatively large extent. This reactive component has little effect in grounds with an impedance higher than  $1 \Omega$ .

### 2.2 Fall of potential Method

This method is applicable to all types of measurements and it has several variations. The figure 12 shows the main test set up for measuring the resistance of a ground electrode system. It is made up from a tested electrode E where is injected the current that flow through it and the current electrode C, after a voltage measurement is made between tested electrode and the potential electrode P in the order to analyze the variations of potential earth according to the distance  $x$  between the two electrodes E and P.

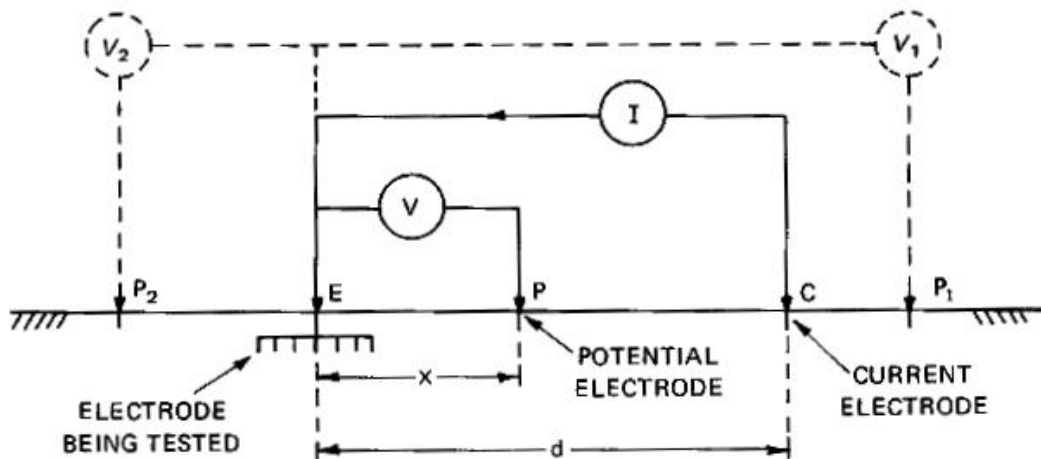


Figure 12 Fall of Potential set-up ( Reproduced from [2] )

The potential profile along the C, P, E, direction will look as in figure 13. Potentials are measured with respect to the ground under test, E, which is assumed for convenience at zero potential

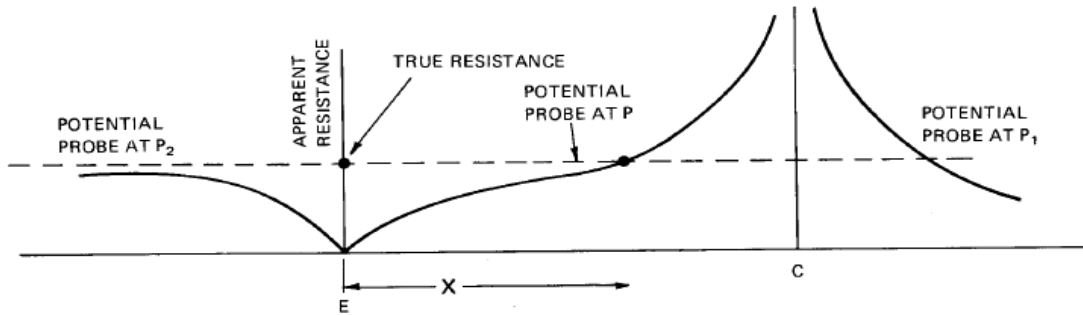


Figure 13 Potential profile along C,P,E direction ( Reproduced from [2] )

From the measurements it is possible to plot the ratio between voltage and current, for each measure correspond to a value of resistance that varies depending on the position of the voltage electrode. As shown in figure 14 we can notice, the curve appears to level out to a value that is assumed as the earth resistance under test.

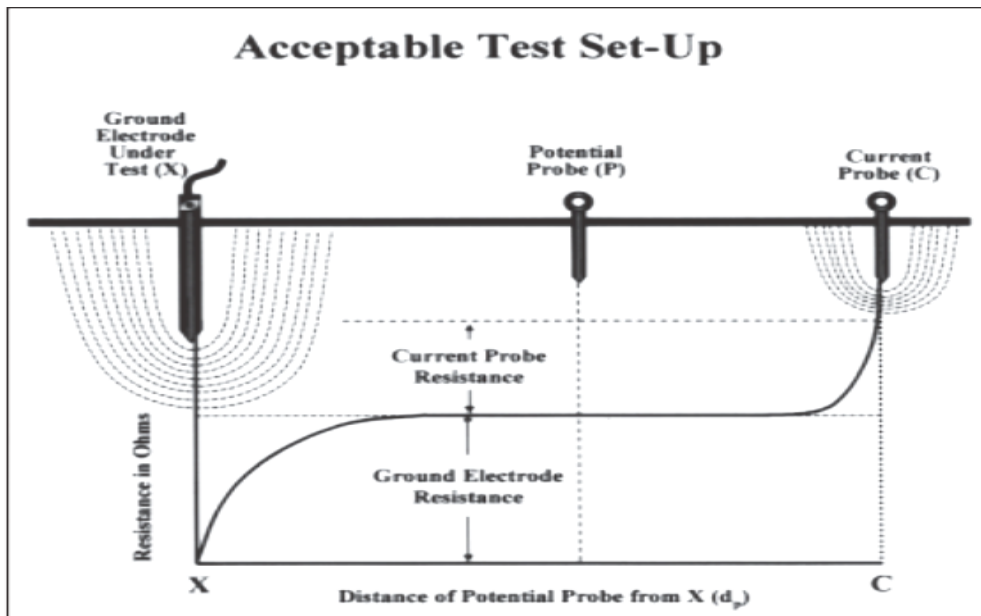


Figure 14 Earth resistance curve with plateau region ( Reproduced from [9] )

In order to obtain a flat portion of the curve is necessary consider the possibility for the current electrode of be influenced from ground to be tested, so the two electrodes E and C must be enough distance to avoid this influence. This influence is sometimes called “extent “of station ground and may be considered as the distance beyond which there is a negligible effect on the measured rise of ground voltage caused by ground current. Ideally, the influence extends to infinity, but practically there is a limit.

If it is not possible to obtain sufficient electrode separation between the electrode under test and the current electrode, a clear plateau region will not appear on the fall-of potential curve, this is due to the ground electrode under test and probe C influences as shown in figure 15.

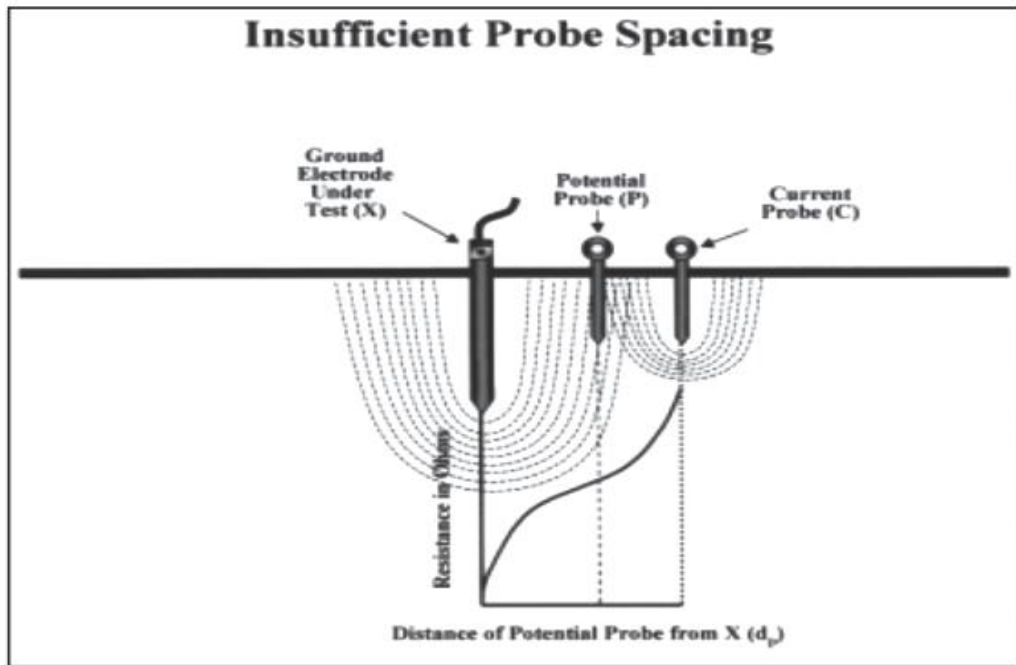


Figure 15 Earth resistance curve without plateau region ( Reproduced from [9] )

In this case to address this problem has been developed an analytical model of the FOP method. The model was based on hemispherical model shaped test electrode of radius  $r$  in uniform earth, and it was shown that the apparent resistance at any one distance  $P$  is equal to :

$$R = \frac{\rho}{2\pi} \left[ \frac{1}{r} - \frac{1}{P} - \frac{1}{C-r} + \frac{1}{C-P} \right] \quad (4)$$

With the approximation that  $r$  is small compared with  $C$ , the solution of Equation 4 which yields the earth resistance of hemispherical electrode  $R = \rho/2\pi r$  is given by condition  $P = 0.618C$ . This method of analyzing the Fall-of Potential curve is therefore known as the 61.8 per cent rule. [5]

It is possible estimate the earth impedance by selecting a particular point for measuring the voltage. The correct position is depending from structure of the soil. In the case of soil uniform, the ratio  $x/d$  is of 0.618, this rule of thumb is applicable if :

- A fairly uniform soil
- Large spacings so that the electrodes may be assumed hemispherical.

The figure 16 shows the required potential probe spacing  $x$  (when the probe is between E and C) for different structure of the soil. indicates, it valid for small ground systems .

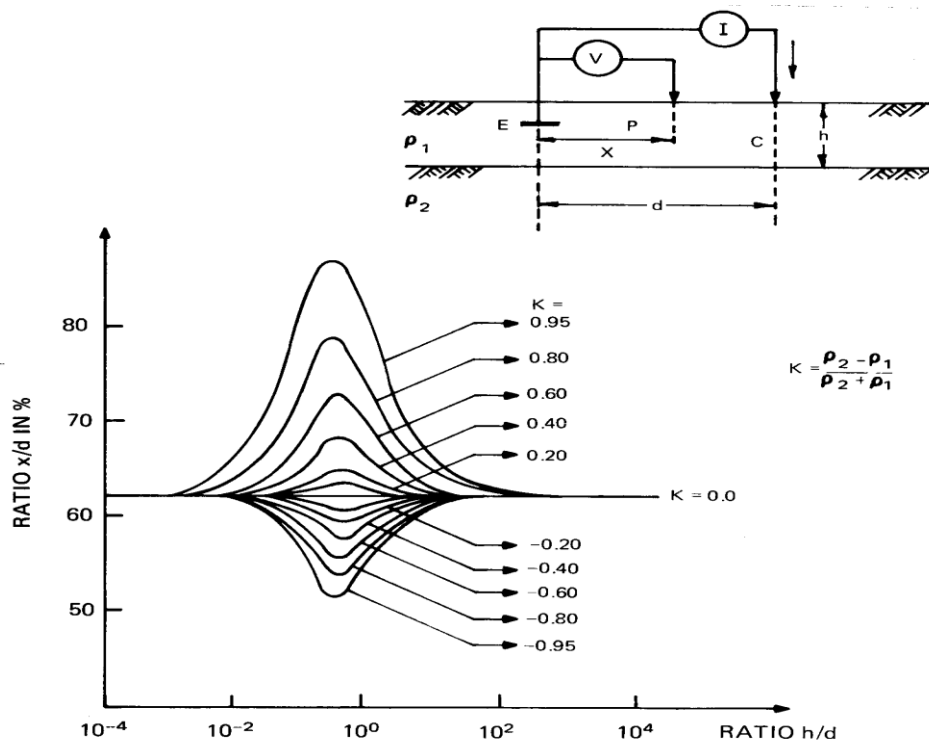


Figure 16 Required Potential Electrode Position in a Two Layer Earth

To get acceptable date of grounding resistance/impedance, about a precision of 95%, must be check the position of the current and potential probe. It will must be at least by 6.5 times the extent of the grounding system. The extension for a grounding system isolated is the maximum diagonal distance, while other external buried conductors are connected with it, therefore add the effective length of buried conductor if in one direction or add every length buried conductor if in opposite direction.

It is important to note at this stage that theoretical analysis of the fall of potential problem shows that placement of the potential probe P at the opposite side with respect to electrode C(P<sub>2</sub>) will result always in a measured apparent resistance smaller than the true resistance. Moreover, when P is located on the same side as electrode C but away from it (P<sub>1</sub>), there is a particular location which gives the true resistance. It should be emphasized, however, that the P<sub>2</sub> arrangement presents the advantage of minimizing the coupling problem between test leads. If reasonably large distance between P<sub>2</sub> and C are achieved ( with



respect to the electrode E under tests), then it is possible to use this method to obtain a lower limit for true resistance of electrode E.

As general conclusion, the best guarantee of satisfactory measurement is to achieve a spacing such that all mutual resistances are sufficiently small and fall of potential curve levels out. The main advantage of the fall of potential method is that the potential and current electrodes may have a substantially higher resistance than the ground being tested without significantly affecting the accuracy of the measurement.

### 2.3 Measurement error for the Fall-of Potential method

The fall of potential method inherently can introduce errors due to :

- Earth mutual resistance due to current flow through earth from the grid to the current probe
- ac mutual coupling between the current test lead and potential test lead
- ac mutual coupling between the extended ground conductor and the potential test lead

#### 2.3.1 Measurement Error Due to Earth Mutual Resistances

Errors of measurement of the grounding-system impedance for mutual resistances can be found from the mutual resistance between the grid and the potential probe, the mutual resistance between the current probe and the potential probe, and the mutual resistance between the current probe and the grid.

These errors can be mitigated by right position of the components concerned as already mentioned earlier in 2.2.

In homogenous earth and for probe spacing one grid diagonal or greater, the measurement of the error due to earth resistance mutual is given by :

$$Re = \frac{\rho}{2\pi} \left[ \frac{1}{\sqrt{C_1^2 + P_1^2 - 2C_1P_1 \cos \phi_1}} - \frac{1}{C_1} - \frac{1}{P_1} \right] \quad (5)$$

where :

- $C_1$  = distance grid center to current electrode, in m
- $P_1$  = distance grid center to potential electrode, in m
- $\phi_1$  = angle between C1 and P1, in degrees
- $\rho$  = earth resistivity, in  $\Omega \cdot m$

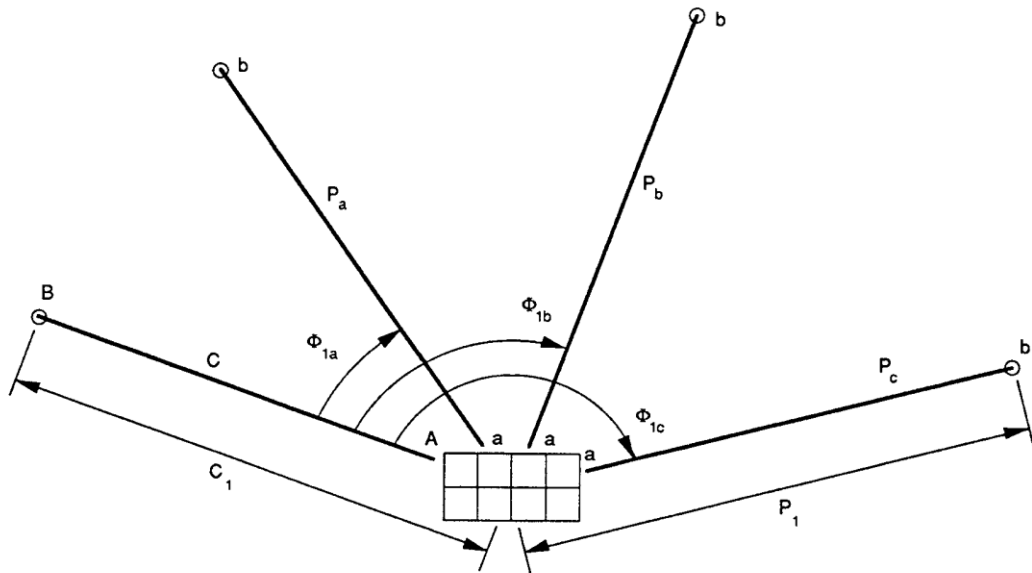
The mutual earth resistance,  $R_e$ , will reduce to zero for a grid installed in homogeneous earth, when

$P_1$  and  $C_1 >$  maximum grid dimension, and

$P_1 = 0.618 C_1$  and  $\phi_1 = 0^\circ$ , or

$P_1 = 1.618 C_1$  and  $\phi_1 = 0^\circ$  or

$P_1 = C_1$  and  $\phi_1 = 29^\circ$



- $P_a$  = POTENTIAL TEST LEAD LESS THAN  $90^\circ$  FROM CURRENT TEST LEAD
- $P_b$  = POTENTIAL TEST LEAD  $90^\circ$  FROM CURRENT TEST LEAD
- $P_c$  = POTENTIAL TEST LEAD GREATER THAN  $90^\circ$  FROM CURRENT TEST

Figure 17 Possible Potential Test Lead Routings Relative to That of the Current Test Lead (Reproduced from [3])

However, for a grid or grounding system buried in heterogeneous earth, containing externally routed ground conductors connected to the grid, these simplifying conditions are, at best, only approximate.

### 2.3.2 Measurement Error due to AC Mutual Coupling

Another source of error in the measurements is the inductive coupling between the current and potential leads, can produce an induced voltage on the potential test lead due to the current that flows on the current test lead. This problem is felt mostly when the test conductors are parallel, in this case the magnetic flux is maximum. The possibility of routing the test conductor with an angle of  $90^\circ$  between them isn't always realizable.

As shown in figure 17 the potential rise measured with the potential conductor  $P_b$  will not be affected from error, while we can't say it for the other two potential conductors,  $P_a$  and  $P_c$ . The induced voltage can produce an increase or decrease of the real tension measured, this depends by the angle between the two test leads. If the angle is less than  $90^\circ$  there will be a

increase of tension at the real value, giving a rise of measured impedance ,while if the angle is more of 90 ° at the contrary there will be the opposite effect so with a reduction of the measured impedance.

The errors recently viewed in these two last items are included in measuring grid impedance, as show in the next equation

$$Z_s = Z_g + Z_M + R_e \quad (6)$$

$Z_g$ = actual grid impedance, in  $\Omega$

$Z_M = R_M + jZ_M$  mutual coupling between  $C$  and  $P$ , in  $\Omega$

$Z_s$  = measured impedance and impedance angle, in  $\Omega$  and degrees

Its value can be substantial, especially for low-impedance value. With frequencies of 60 Hz can have mutual couplings which are about 0.1  $\Omega$  /100 m. Low impedances usually there are when requires long test leads to reach remote earth . Contrary the small areas the problem there is not because I have to do with high impedance and conductors short to reach remote earth. As a rule of thumb test lead coupling is usually negligible on measurements of grounds of 10  $\Omega$  or greater, is almost always important on measurements of 1  $\Omega$  or less, and should be considered in the range between 1 and 10  $\Omega$  .

### **2.3.3 Mutual Coupling to Potential Lead Extend Ground Conductors**

As mentioned 2.3 large grounding systems may include buried neutral, overhead neutrals, overhead ground wires, control and communication shields, water pipes, gas lines, and railroad tracks. Viewed the extent and the complexity of these ground conductor may be difficult find a right routing for the potential test lead without the introducing measurement error.

## **2.4 Practical testing considerations**

These kind of measurements , earth resistivities, ground impedances, and potential gradients are more complicated than other resistance, impedance, and potential measurements. It may be necessary to make multiple measurements and to plot trends.

The factors that influences the measurements are :

- Test electrodes
- Stray currents
- Coupling between test leads (see section 2.3.2 )
- Buried metallic objects
- Background noise

Nowadays with the development and industrial growth adjacent to power substations, it becomes increasingly difficult to choose a suitable direction or locations for the test probes to make a resistance test. Partially or completely buried objects as rails, water or other industrial metallic pipes will considerably influence, whenever the presence of these buried objects is suspected in the area where soil resistivity measurements are to be taken and the location of these structures is known, their influence can be minimized by aligning the test probes in a direction perpendicular to routing of these structures. Also the location of the test probes should be as far as possible from the buried structures.

In the measurements if the method used is the Fall of Potential Method, theoretically the ground resistances of the test electrodes do not influence the measurements since these are taken into consideration by the method of measurement .

However the value of resistance of the electrodes should not exceed a maximum value beyond the test current can get insufficient to be measured with the instrumentation available. By insufficient test current is meant :

- 1) Current lower than instrument sensitivity
- 2) Current in the order of magnitude of the stray currents in the earth

For the first case an answer to a problem is possible by increasing of the test current, it means to increase the voltage of the power supply or by decreasing the test electrodes resistances. The choice of using a decrease in resistance of the electrodes is certainly easier to apply. The availability to have an adequate power supply is not always obvious, then there are limits beyond which enter into account safety aspects. The decrease of the test electrode resistances can be done by driving the rods deeper in the ground, pouring water around it or adding other rods connected in parallel. In general the value of the electrodes should meet the requirements of the instrumentation used. With commercial instruments a potential electrode resistance of  $1000\ \Omega$  can be used, some allow the use up to  $10000\ \Omega$ . Concerning the electrode current its value should be about the  $500\ \Omega$  . This value is a function of supply voltage and current required, indeed the ratio between generated voltage and the test electrode resistance determines the current generated. As a rule of thumb the ratio between the current electrode resistance and the ground resistance being under tested should never exceed 1000 to 1, preferably 100 to 10 or less.

About the second case, when dc tests are being made, the test current must be increased to overcome the interfering effects of stray dc earth currents. When tests with ac or periodically reversed dc signals are being made, the frequency of the test signal may be set to a frequency not present in stray currents. Most measuring devices use frequencies within a range of 50 Hz to 100 Hz. The use of filters or narrow band measuring instruments, or both, is often required to overcome the effects of stray alternating currents.

The background noise arises from unbalanced loading on the three-phase system, the presence of harmonics or any other mechanism that causes a current through the grid. This noise can be quantified by the standing voltage present on the earthing system with respect to remote earth and the magnitudes are typically in the range from 100mV to several

tens of volts. The background noise can be measured using frequency-selective voltmeter or a spectrum analyzer. [5]

## **2.5 Behaviour of earthing system under high frequency**

Earthing systems in distribution and transmission networks are designed to provide adequate safety levels under normal operating and fault conditions. It is well known, however, that designs made for power frequency operation have a different response under high frequency and transient conditions. Such conditions arise during fault and switching transients as well as when the system is subjected to lightning strikes. [11]

IEEE Std. 80 (Guide for safety in substation grounding) does not provide detailed guidance for designing earthing systems subjected to lightning surges but considers that grounding systems designed according power frequency principles will “ provide a high degree of protection against steep wave front surges...” This is based on assumption that the human body can withstand higher current for very short duration. [5]

The standardized method adopted to characterize the earthing systems doesn't need particular considerations about the behaviour of the earthing system under the test conditions. This is because particular phenomena such as soil ionization does not appear. Therefore the earthing systems are usually seen as pure resistance. This is not true however, when the earthing system are tested under high frequency or impulse.

The performance of earthing systems under transient conditions is different from power frequency behaviour because of more significant influence on inductive and capacitive effects. In contrast to the 50 Hz response, at high frequency the inductance of a small earthing system, such a rod, has a significant effect and the effective length of such systems can be very small.

The figure 18 shows the frequency response of a 100 by 100 m<sup>2</sup> earth grid for a range of soil resistivities. As can be observed, each curve has a lower frequency range over which the impedance is nearly constant. For each earth resistivity value, the impedance increases rapidly above a threshold frequency, and this behaviour can be attributed to the inductance of the conductor.

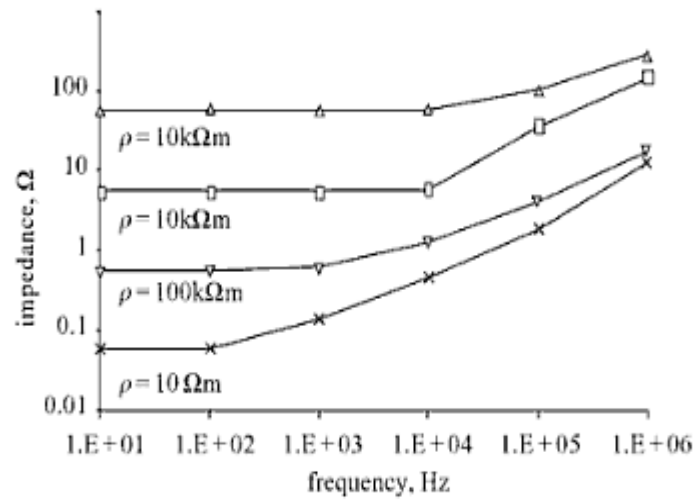


Figure 18 Earth impedance of a grid as a function of frequency for different soil resistivities

### 3. Measurements Using the Fall-of –Potential Method

In this section we will evaluate the influence, the variations, of the inductive mutual coupling between leads with the use of the classical fall of potential. The value of frequency used, of the type of soil, the distance between the current and potential leads, grounding system size will have a influence on the magnitude of mutual coupling, hence the value of the ground impedance measurements

This problem is more felt for large grounding system , essentially for two motives :

- is required a long distance between the current probe and the grounding system
- it has generally a small impedance value, therefore a lower tolerance to the noise

The effect of the mutual coupling is higher with the increase of the frequency, could use low frequency or even work with DC and in trade there are some modern low frequency resistivity/resistance meters but it lack of a high capacity to generate test current for large spacing between the current probe and the grounding system to overcome the high noise levels which can develop at such spacing.

In the following sections, different scenarios showing the influence of inductive coupling on ground impedance.

#### 3.1 Uniform Soil

In the follow figure 19 is shown a plan of the ground impedance measurement setup based on fall of potential method .

Its features are :

- size grounding system = 100 m by 100 m and 16 mesh
- buried depth = 0.5 m
- soil resistivity = 100  $\Omega$ -m
- radius the grid conductor = 0.5 cm
- distance between current probe and grid = 1000 m

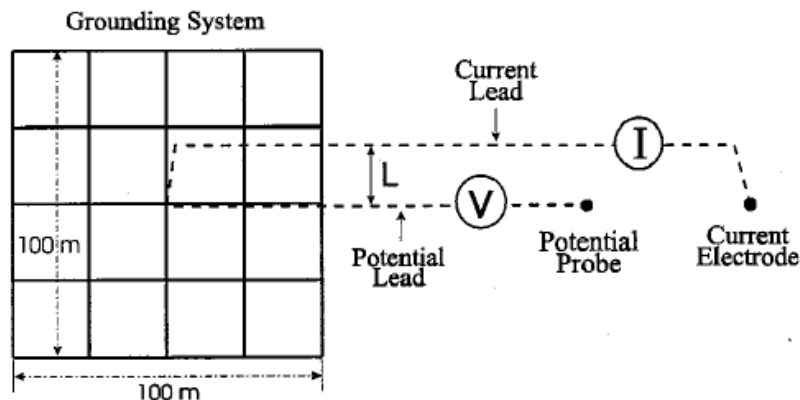


Figure 19 Plan view of the ground impedance measurement setup (Reproduced from [4])

### 3.2 Different Lead Separation Distances

In figure 20 are shown computed three different curves, without mutual coupling, and two cases with the distance  $L$  between the current and potential leads of 1 m and 10 m, the operating frequency is 80 Hz. The case without mutual coupling reflects the real value of the ground impedance. The right location of the potential probe is  $X = 0.618$ , and we can see that the correct value measured is  $0.523 \Omega$ . With a distance  $L$  of 1 m and 10 m we will have respectively a value of  $0.668 \Omega$  and  $0.601 \Omega$  and hence a relative error of 28% and 15%. We can figure out that more is high the distance between the two leads and less will be the effect of the mutual coupling. A management of the problem with the increase of  $L$  is often probably impracticable, due the property lines or physical obstacles.

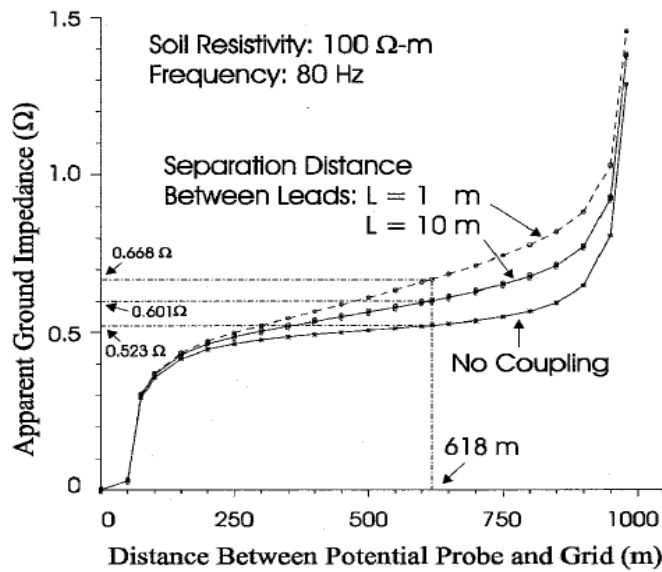


Figura 20 Simulated Fall-of-Potential measurements (Reproduced from [4])

### 3.3 Low Resistivity Uniform Soils

In this section we evaluate the influence of resistivity earth on the mutual coupling. The figure 21 shows the computed Fall of Potential curves, without mutual coupling, with the distance  $L$  of 10 m and 1 m. The resistivity soil in this case is of  $10 \Omega\text{-m}$  instead  $100 \Omega\text{-m}$ ; the operating frequency is still 80 Hz and  $X = 0.618$  m.



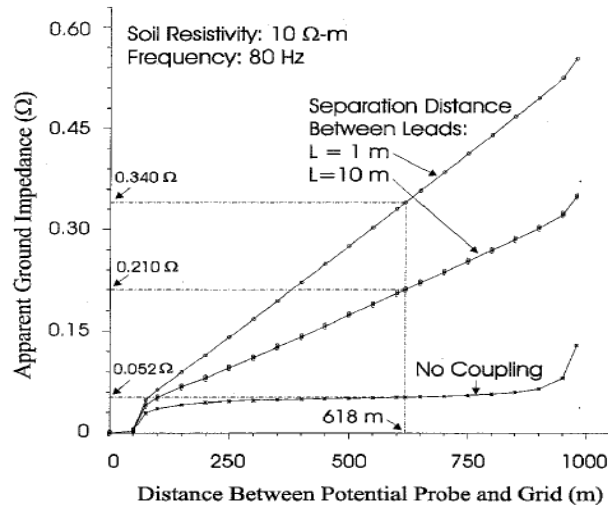


Figure 21 Simulated Fall-of-Potential measurements (Reproduced from [4])

The measured ground impedances with inductive coupling are 0.210 for the 10 m separation and 0.340 for the 1 m separation, resulting in relative errors of 304% and 554%, respectively, which are extremely large compared to 15% and 28% for a 100 Ω-m uniform soil. The reason for the strong influence of inductive coupling in low resistivity soils is that the meaningful signal decreases proportionately to the soil resistivity, while the induced voltage is much less sensitive to the soil resistivity and therefore decreases much less than the signal.

### 3.4 High Operating Frequencies

In this section we evaluate the influence of the operating frequency, the parameters are the same of the first case, the only differences is that the operating frequency is of 500Hz.

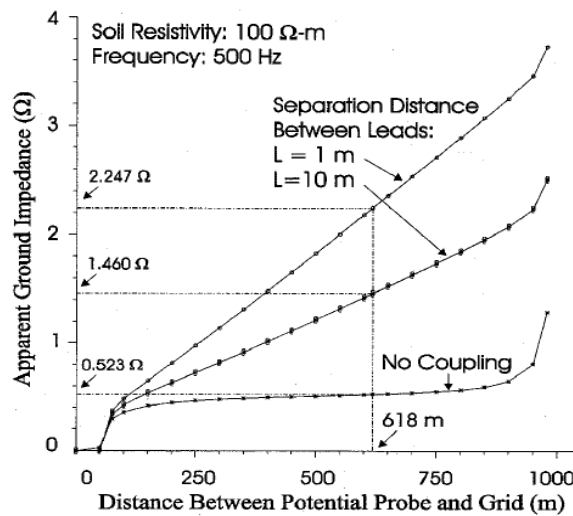


Figure 22 Simulated Fall-of-Potential measurements (Reproduced from [4])

The influence of inductive coupling on ground impedance measurement at this frequency is clearly much larger than that at 80 Hz. The measured ground impedances with inductive coupling are 0.210 for the 10 m separation and 0.340 for the 1 m separation, resulting in relative errors of 304% and 554%, respectively, which are extremely large compared to 15% and 28% for a 100 -m uniform soil.

### 3.5 Small Grounding Grid

In the section the our grounding system has a different size, is smaller than before, 50 m by 50 m 16- mesh. Are examined two cases, the influence of frequency figure 23 and soil resistivity figure 24 . The figure 23 shows the value of ground impedance for  $L= 1$  m for a frequency of 80 Hz and a frequency of 500 Hz.

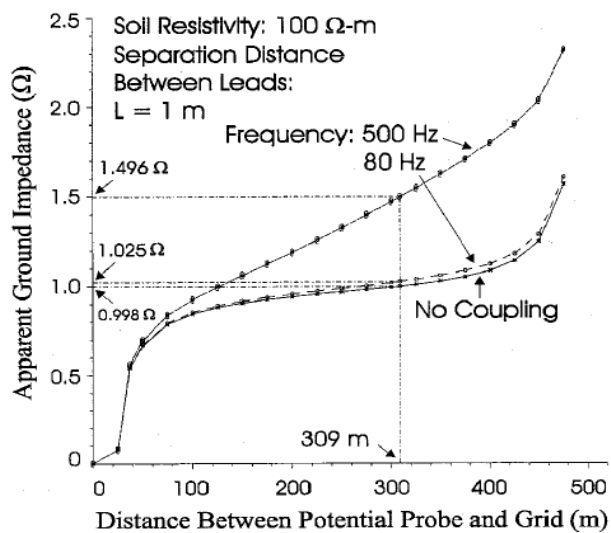


Figure 23 Simulated Fall-of-Potential measurements (Reproduced from [4])

For this smaller grid, the influence of inductive coupling on ground impedance measurements at 80 Hz is very small. At 500 Hz, however, the relative error of the measured ground impedance is still relatively high (50%) even for this small grid.

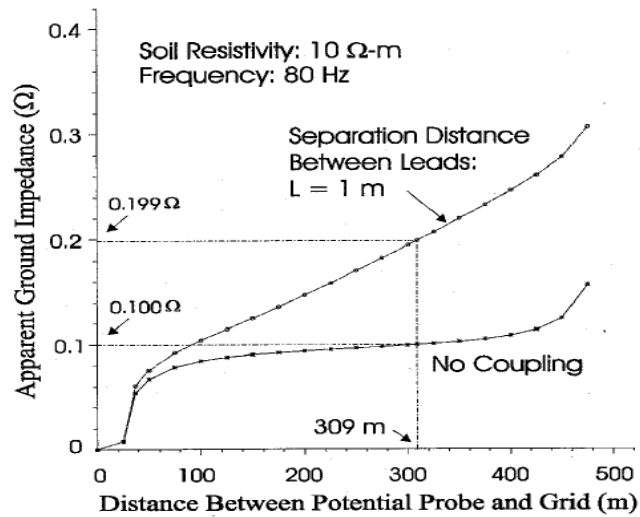


Figura 24 Simulated Fall-of-Potential measurements (Reproduced from [4])

It can be seen that the relative error of the measured ground impedance is about 100%, which is not acceptable. The results in this section show that generally, ground impedance measurements for small grids are less susceptible to inductive coupling than for large grids. However, the inductive coupling may not be negligible when the operating frequency is high or the soil resistivity is low.

### 3.6 Conclusions

The variation of the influence of inductive coupling between leads with soil, resistivity, grid size, lead separation, operating frequency and different soil structures has been modelled and analyzed. The results shows that when the operating frequency is high or the soil resistivity is low or the grounding grid is extensive, the measurement results are more severely influenced by inductive coupling than otherwise.



## 4 Carson-Clem method and Complex-image method

### 4.1 Introduction

Almost all methods for measuring grounding systems impedance are based on current flows between the grid under analysis and the current probe, while the grounding potential rise (GPR) is measured between the grid and potential probe. This set up as mentioned above involves a mutual coupling between the current and potential leads and than an error in the measurement. A calculation of grounding systems impedance, especially for large systems and non-uniform soil, it is not reliable as a measurement. Have a knowledge of which is the mutual coupling is indispensable, for this reason a comparison between Carson-Clem formula and Complex-Image formula was conducted to evaluate and looking at what are the characteristic that distinguish.

### 4.2 Carson's formula

The study of the mutual coupling is made by Carson theory. The Carson's formulas are based on the following assumptions :

- 1) The inducing line is a horizontal straight conductor of infinite length in which flows a constant current.
- 2) The lines, between which the mutual impedance is to be calculated, are parallel to each other.
- 3) The earth is homogeneous of finite resistivity.

These assumptions are valid only for the basic case and with specific cases the relationship and values concerning the basic case should be modified in the appropriate way or new methods should be established for deriving the mutual impedances.

- 1) The effect of parallel lines of finite length which acts when the inducing line is relatively short, is a such case : the concentration of the earth current in the vicinity of the earth electrodes can no longer be neglected and the so-called " end effects" must be in consideration. This can be done by introducing the finite length values of inductance.
- 2) The effect of oblique exposures and crossings lines
- 3) The effect of stratified earth

The expressions used in both methods are derived from the Carson/Pollaczek theory with reasonable simplifications.

The Carson's formula for mutual impedance, per unit length, composed of the following expression :

$$Z_{ij} = j\omega \frac{\mu_0}{2\pi} \ln \frac{D_{ij}}{a_{ij}} + j\omega \int_0^{\infty} \frac{2e^{-(h_i+h_j)\lambda}}{\lambda + \sqrt{\lambda^2 + j\omega\mu_0\sigma}} \cos \lambda d_{ij} d_{ij} \quad (7)$$

where:

$$j\omega \int_0^{\infty} \frac{2e^{-(h_i+h_j)\lambda}}{\lambda + \sqrt{\lambda^2 + j\omega\mu_0\sigma}} \cos \lambda d_{ij} d\lambda = 2(\Delta R_{ij} + \Delta X_{ij}) \quad (8)$$

The formula consists of two terms:

- the first is a geometrical term, it would give the impedance for the case of a perfectly conductive earth.
- the second part of the equation is the correction term which takes into account the finite conductivity of the earth, it has generally higher value than geometrical term.

A numerical integration for the evaluation of the second term is preferably to be avoided even with by computer. Various methods have been developed to deal with this in practice, as Carson- Clem formulas, Polynomial form, image Complex formulas, form series, each of which is more suitable depending on the applicability and instrumentation used.

#### *Nomenclature*

$\rho$ = resistivity of the earth [ $\Omega$ -m]

$f$ = frequency of the inducing current [Hz]

$\omega = 2\pi f$  angular frequency of the inducing current

$\mu_0 = 4\pi \cdot 10^{-7}$  permeability of free space

$D_e = 659 \sqrt{\frac{\rho}{f}}$  equivalent depth of hypothetical return path of the earth current

$a_{ij}$  = separation (horizontal distance) between conductors i and j

$h_i$  and  $h_j$  =height above the ground-level of conductors i and j respectively,( if a conductor is underground its height has negative value)

$d_{ij} = \sqrt{a_{ij}^2 + (h_i - h_j)^2}$  distance between conductors i and j

$$\alpha = \sqrt{\mu_0 \frac{\omega}{\rho}} = 2.809 \cdot 10^{-3} \sqrt{\frac{f}{\rho}}$$

$x = \alpha d_{ij}$

### 4.3. Carson-Clem formula

A easily and practice way to evaluate the mutual impedance is been developed. Carson-Clem formula is applicable in all cases where the product of  $\alpha$  and  $d_{ij}$  is less than 0,25 and the height of the conductors above the surface of the earth is also small compared with the wavelength. The Carson-Clem formula is derived from the Carson's formula by the following assumptions:

- the geometrical term is neglected,
- the terms considered from the Carson's series expressions are only the first term of  $\Delta R$  and two term from  $\Delta X$

The mutual impedance can be calculated as a function of  $x$  from the following expression:

$$Z = 10^{-3} \left( 0.157\omega + j\omega 0.2 \ln \frac{1.852}{x} \right) \quad [\Omega/km] \quad (9)$$

The Carson-Clem formula for mutual impedance is obtained from the formula 9 by using  $x=\alpha d$  and  $D_e$ :

$$Z_{ij} = \left( 10^{-3} * 0.99f + j\omega 2 * 10^{-4} \ln \frac{D_e}{d_{ij}} \right) [\Omega/km] \quad (10)$$

In practice the Carson-Clem formula can be applied at those cases where the value of  $x$  is less or equal to 0.25, with a precision of the results lower to 2.5 %.

At the same way is possible to explicate the limit according the resistivity and frequency to find the maximum value of  $d_{ij}$  as following:

$$d_{max} = \frac{0.25}{2.81 \cdot 10^{-3} \sqrt{\frac{f}{\rho}}} = 88.97 \sqrt{\frac{\rho}{f}} \quad [m] \quad (11)$$

While the ratio of  $d_{max}$  and  $D_e$  is :

$$\frac{d_{max}}{D_e} = \frac{88.97}{659} = 0.135 \quad (12)$$

This means that the Carson formula can be applied until the separation between the conductors is less than 15% of the equivalent earth return distance  $D_e$ .

### 4.4 Expression to evaluate the mutual coupling between parallel or angled conductors of finite length

The Carson-Clem method just explained has some limitations, in case of angled leads it cannot apply, a gap for the evaluation of grounding systems impedance. The following method allows the evaluation of the mutual coupling between angled and parallel leads of different or equal length.

As mentioned above the current flows through the conductor and then back to the grid through the ground, it forming a closed circuit. It can be modelled by a perfect conducting plane which is located at complex depth  $p$  below the earth surface, as shows the figure 25.

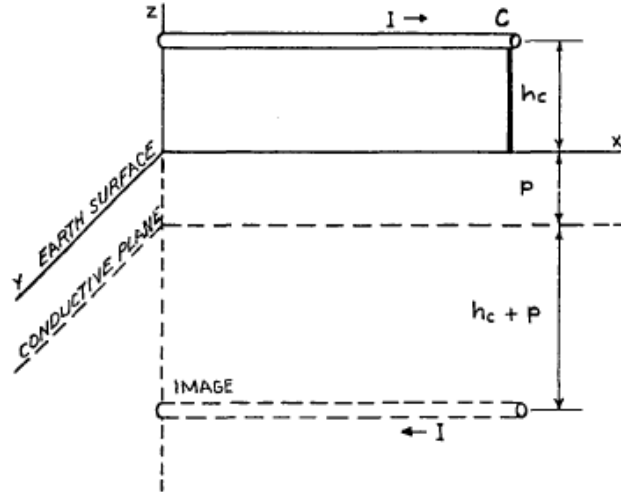


Figure 25 Ground return conductor above homogeneous earth (Reproduced from [7])

The complex depth  $p$  is give from :

$$p = \frac{1}{\sqrt{j\omega\mu_0\sigma}} \quad (13)$$

where:

$$\sigma = 1/\rho$$

By the method images the conductive plane can be replaced with a conductor at a depth  $h_c + 2p$  below the earth surface. By using this model and Neumann's integral is possible to calculate the mutual coupling between the conductor C which creates the direct mutual coupling and the conductor C placed at height  $h_c$ , at the same way calculate the indirect mutual coupling between P and the image conductor.

Considering a homogenous earth, the diameter of conductors is very small, the current is constant along the entire length and the vertical connections between the conductors and the ground are very short compared with the conductor length, the total mutual coupling is given by :

$$Z_M = R_{M+}X_M = j \frac{\omega\mu_0}{4\pi} (M_d - M_i) \quad (14)$$

Where  $M_d$  and  $M_i$  changes depending on whether the conductors are parallel or angles, as shown in appendix

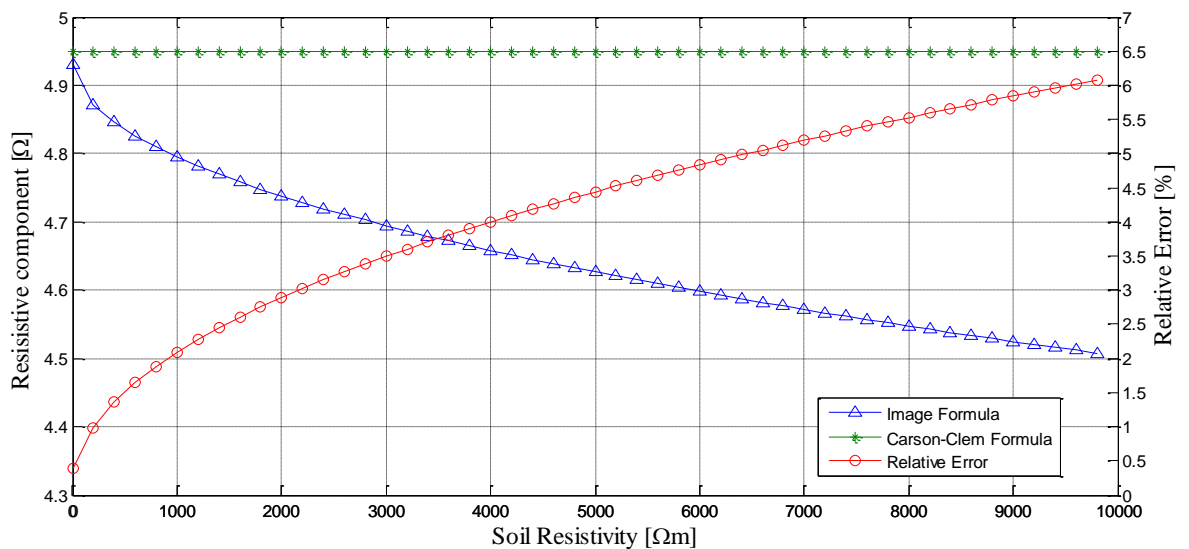


#### 4.5 Comparison between Complex-image method and Carson-Clem method

A comparison of Complex-Image method and Carson-Clem Method was performed by using Matlab, in order to evaluate the relative error to vary of the soil resistivity, frequency, length of the leads and their separation. As standard was used the Carson-Clem Method, taking into account that it has an accuracy in the evaluation of mutual coupling between two conductors of 2.5% ,if the parameter  $x$  is less than 0.25. For each simulation was evaluated the resistive and reactive component of mutual coupling, with the potential and current leads at the same length and parallel between them.

The first simulation is based on the soil resistivity, as shown in the figures 26-a and 26-b. The following data have been considered:

- length of the leads : 100 km
- frequency: 50 Hz
- separation: 1 m
- leads lying on the ground



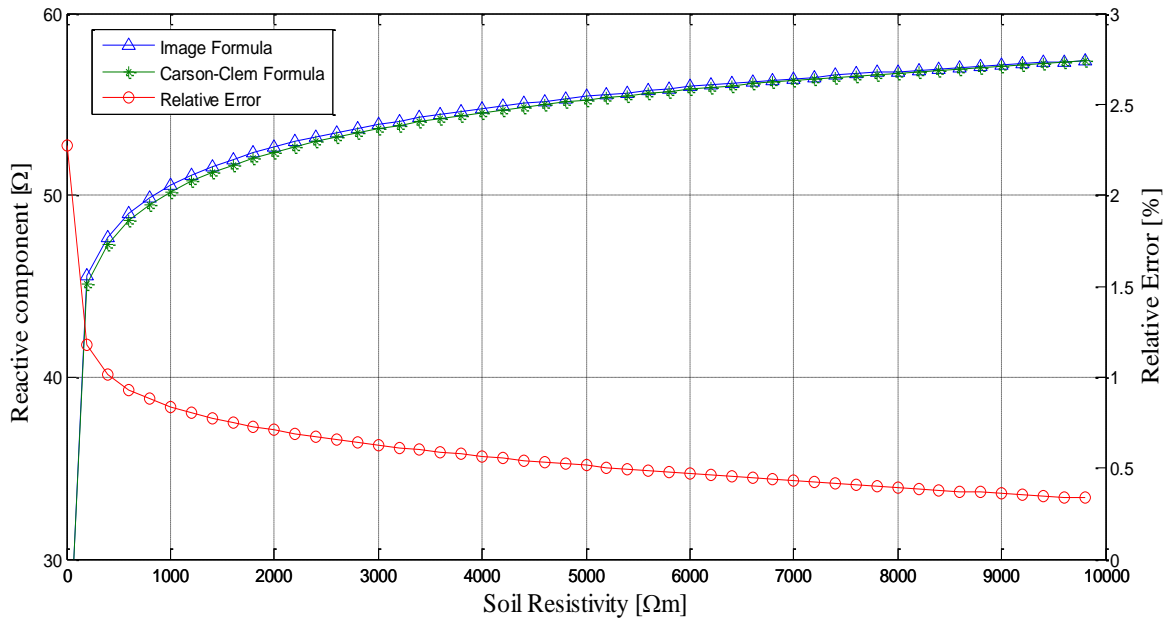


Figure 26-a 26 b Resistive and reactive component as function of the soil resistivity

As the figures 26a-26b show, the relative error has a decreasing trend for the reactive component with increasing of resistivity (it is slightly above the 2% with low resistivity), while for high soil resistivity's values, the relative error is about 1%. As to the resistivity component, there is an increasing trend with a relative error of about 0.5 % for low resistivity, while for high resistivity (around 10000  $\Omega$ -m), the relative error is slightly above the 6%. However this component has a low influence on the mutual coupling magnitude. The accuracy of the Carson-Clem formula is not guarantee for extremely low values of resistivity, however these values are not found normally. In the resistivity interval analyzed the relative error is very low. The complex-image method is applicable independently of the resistivity.

The second simulation is based on the length of conductors, as shown in the figure 27-a and 27-b, by using the following data:

- earth resistivity : 130  $\Omega$ -m
- frequency: 50 Hz
- separation: 1 m
- leads lying on the ground

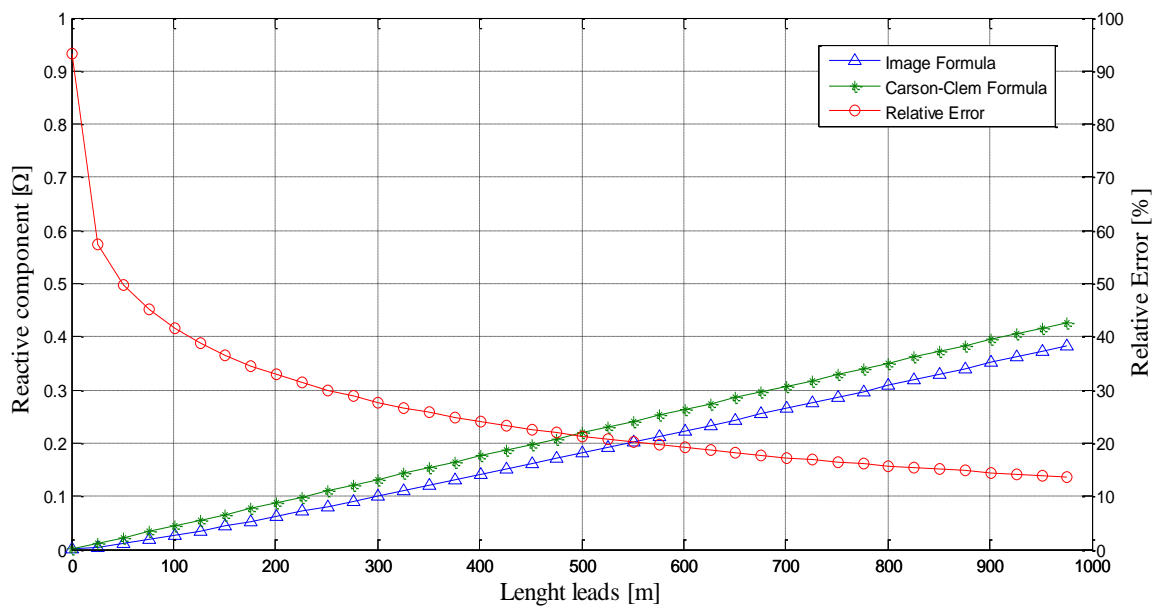
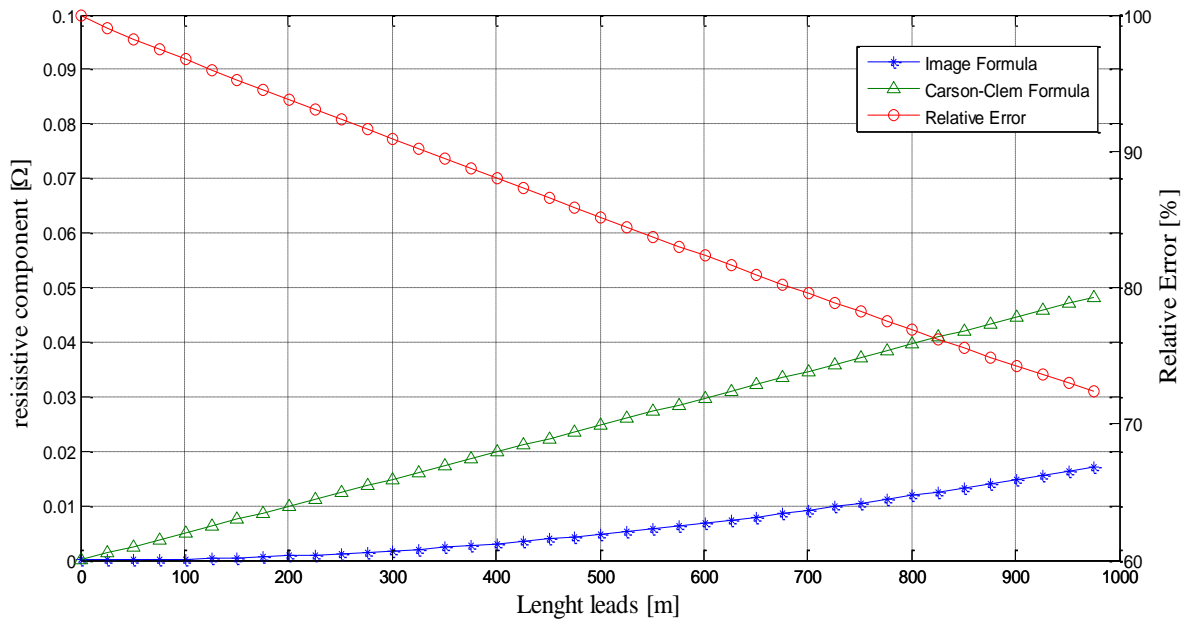


Figure 27-a 27-b Resistive and reactive component as function of the length leads

The relative error for the resistive component varies from 100% to 72%, while in the reactive component it varies from 95 % to 15% for short leads and 1000 m respectively as shown in the figures 27a-27b. In both cases the relative error has a decreasing trend with the increasing of length leads, whereas for the resistive component it remains pretty high. The relative error is negligible in the resistive component, so it has not an important influence over the ac mutual coupling in comparison with the reactive component. It is possible to point out how the Image Formula is not totally suitable for calculating the mutual coupling in case of short length leads. Here the mutual coupling evaluated is reduced respect predicted by Carson-Clem formula probably due to the phenomenon called end-effect. The leads of the length do not influence the accuracy of the Carson-Clem formula.

The third simulation is based on o the frequency, as shown in the figure 28-a and in the figure 28-b ,with the following data :

- earth resistivity : 130  $\Omega$ -m
- length leads : 100 km
- separation: 1 m
- leads lying on the ground

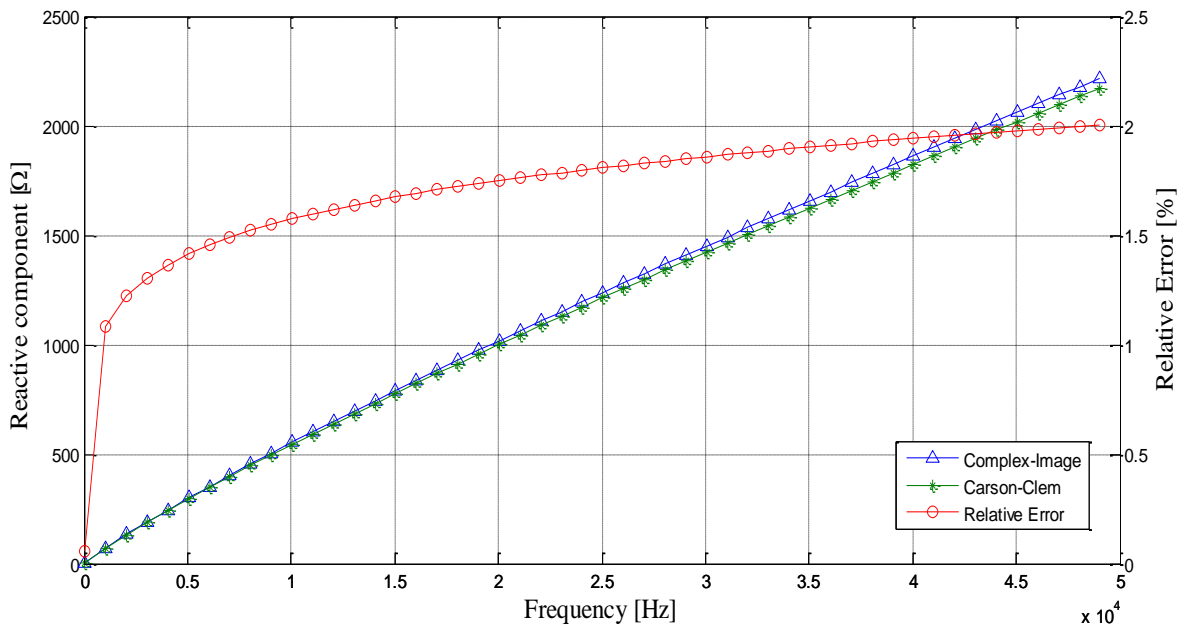
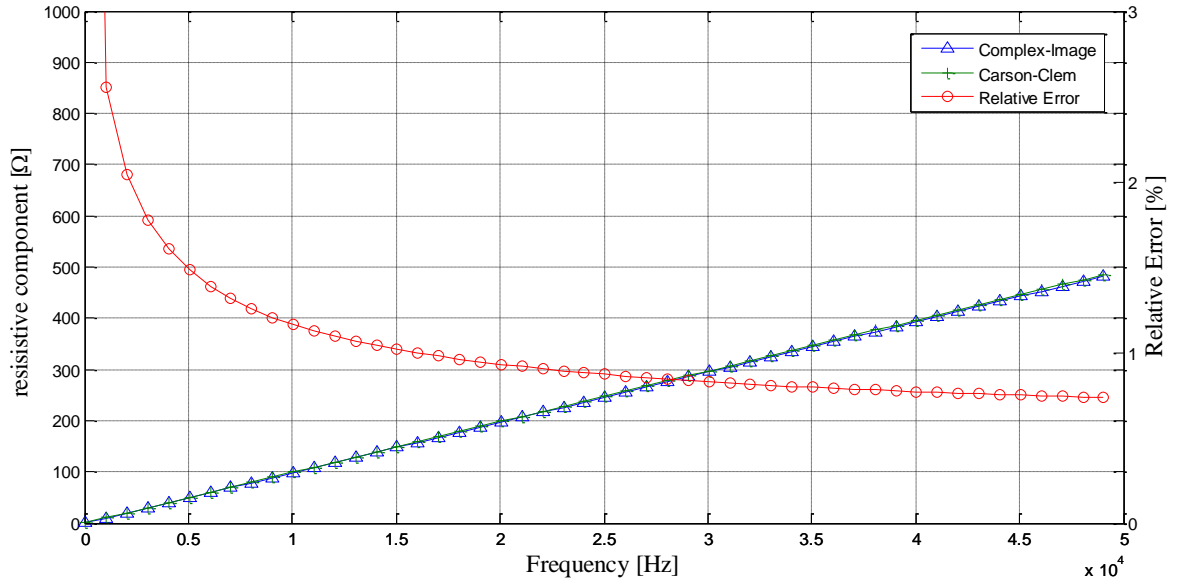


Figure 28-a 22-b Resistive and reactive component as function of the frequency

The simulation was done for a frequency range from 50 Hz to 50 kHz. In the resistive component its relative error has a decreasing trend with the increase of frequency, whereas in the reactive component the relative error has an increasing trend. In all the interval the relative error for both the components is low, it is less than 2%.

As to the accuracy of the Carson-Clem Formula, the maximum frequency applicable is of 100 kHz with the used data, so it is widely higher than the upper limit analyzed.

The fourth simulation is based on the separation distance between leads, as shown in the figure 29-a and the figure 29-b, with the following data:

- earth resistivity : 130  $\Omega$ -m
- length leads : 100 km
- frequency: 50 Hz
- leads lying on the ground

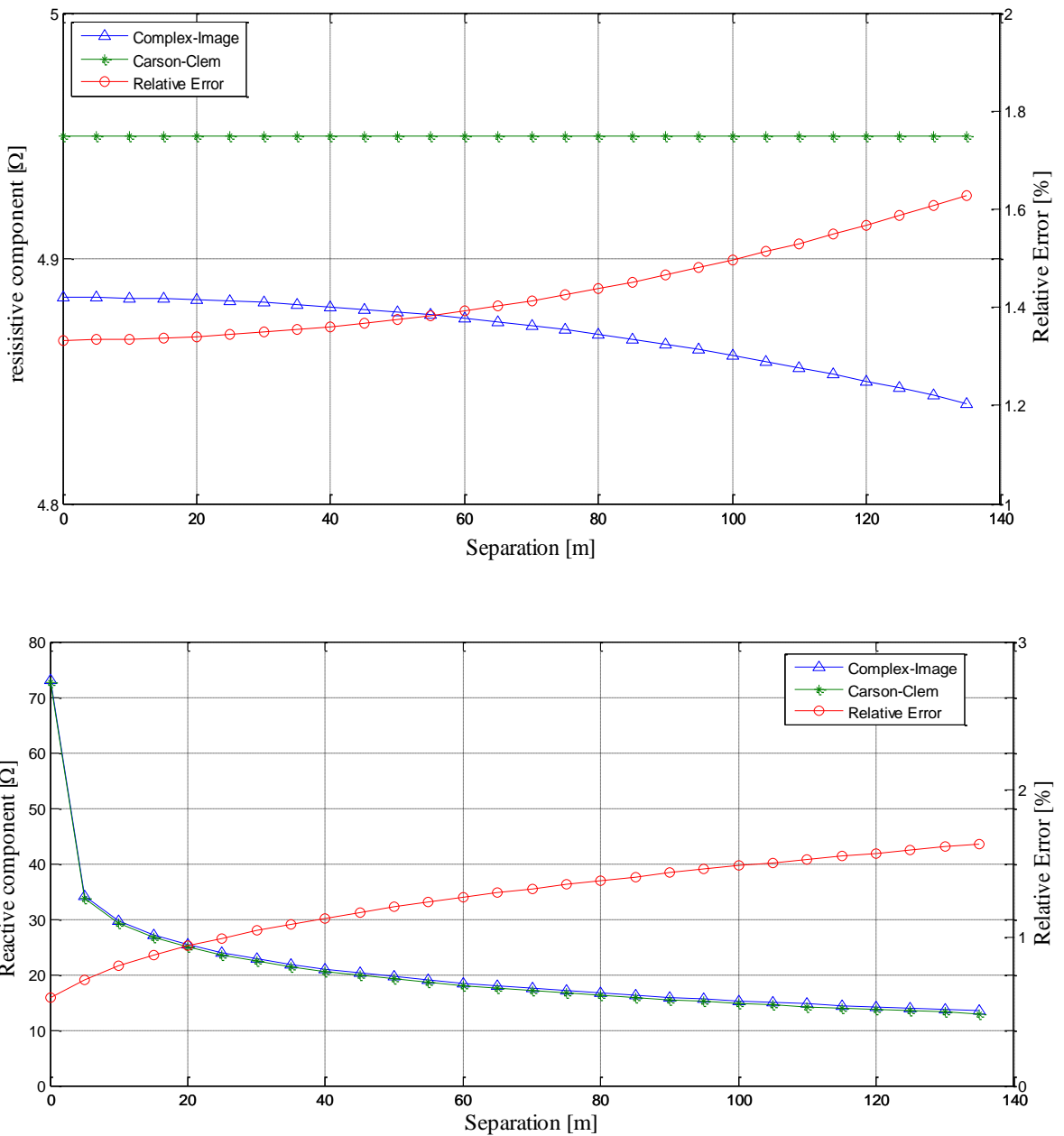


Figure 29-a 29-b Resistive and reactive component as function of the separation

The relative error for the resistive component is less than 1,4% for short separation and about 1,7% for separation of 140 m, therefore with a slow increasing trend. For the reactive component the trend is similar, with a relative error of about 0,8 % and 1,2 % for short and long separation respectively. To ensure the accuracy of the Carson-Clem Formula I used the maximum separation of 140 m. The relative error due to the Complex-Image formula is negligible, considering the interval that was used.

#### **4.6 Conclusions**

Different simulations have been implemented as function of a parameter, with different characteristics that would make the variable under analysis not influenced by the others parameters on the result of the relative error. It is possible to note how the relative error for the Image Formula with Carson-Clem as a standard is relevant when the length of the leads is short. Indeed, in this case, the relative error is pretty high for both the component of the mutual coupling, probably due to the end effects, it is not considerate and it should be taken into account. So it should be advised the use of Carson-Clem Formula in case of short leads. However the Carson-Clem theory is based on leads that have a infinite length, so the mutual coupling can be analyzed for short lengths but only when the background of the parallel lines is considered infinite. The other parameters does not influence significantly the relative error but however the combination of different errors can cause error a higher error than the one we expected, then in each case a specific analysis is recommended.

## 5 Field Tests by using the Fall Of Potential method

### 5.1 Introduction

The tests were carried out at Llanrumeny field, the 20 may 2011, under the supervision of the Dr Huw Griffiths and the Ph.D Salah Mousa.. It was valued the apparent resistance and ac mutual coupling to vary of frequency for a grid 3 m by 3 m buried at depth of 0,5 m.

Three different applications of the Fall of Potential Method were carried out, each of which was simulated by software CDEGS.

The tests were executed with:

- Angled leads, 90 degree
- Parallel leads, separation of 1 m
- Parallel leads, separation of about 6 cm

In the two last tests were estimated the ac mutual coupling between leads to correct the errors in the measurements and simulations. In the first one the leads were angled at 90 degree, therefore this estimation had not been necessary because obviously there is not a concatenate flux between the leads.

### 5.2 Characteristics grid and soil

- Grid :

size	3x3 m
Buried at depth	0,5 m
Rods	Not included
diameter grid conductors	0,671 cm
Total conductors buried	18 m

*Table 1 Characteristics of grid*

- Characteristic soil :

Regarding to the choice of the model to represent the soil I used the investigations of soil resistivity that was carried out by the Ph.D. Salah Mousa. The measurements were estimated at Llanrumney in different positions and moments. I decided to take into account as reference the one that was carried out between the years 2008 and 2010 near where I performed my measurements, as shown in figure 30 .The measurements was carried out by applying Wenner Method and using AMEB meter with various electrode spacing.



Figure 30 Soil resistivity measurement location at Llanrumney field site

The values of apparent resistivity are plotted against the spacing, as shown in the figure 31.

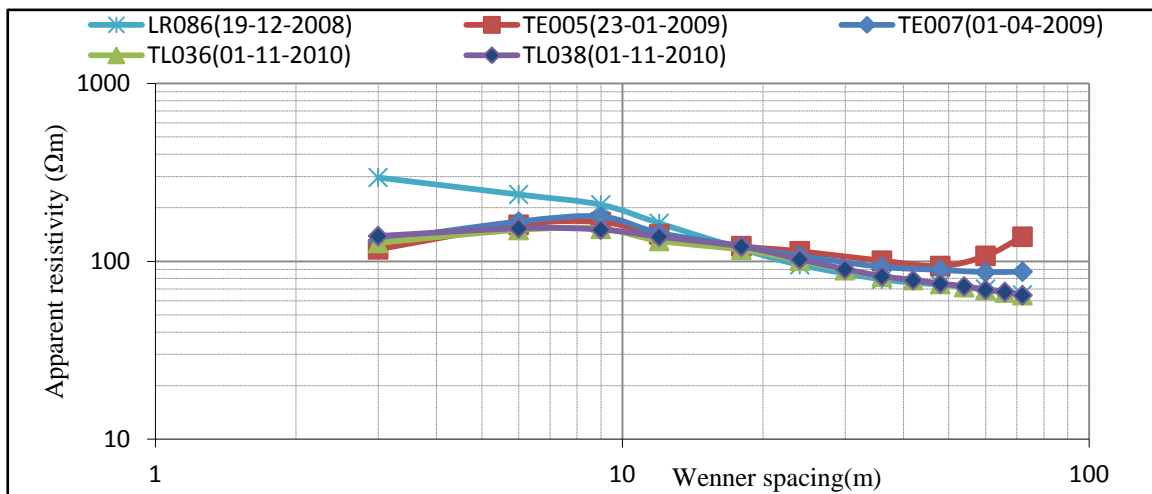


Figure 31 Results of apparent resistivity



The table 2 sums up the apparent resistivity values that were obtained for shortest and longest spacing electrodes in January 2009, April 2009, December 2008 and two values on the same date but at a different place in November 2010.

Soil Resistivity ( $\Omega\text{m}$ )					
Electrode	Dec. 2008	2009		Nov. 2010	
		Jan.	Apr.	Place1	Place2
Shortest	296	116	131	127	138
Longest	65	138	88	65	65

*Table 2 Selected Results of apparent resistivity*

We can see how the resistivity varies widely depending on the spacing electrode for each test. This precludes an uniform model. Furthermore it's important to point up as the apparent resistivity varies depending on the place and on the moment the test was carried out, the latter due to seasonal variations .

To represent the soil I decided to use a model with two layers with different resistivity. The upper layer with a resistivity of  $150\Omega\text{m}$  and a depth of 7 m above a lower layer of an infinite depth and earth resistivity of  $70\Omega\text{m}$ .

Before carrying out the different tests it is important to have an approximate idea of which can be apparent resistance value of the grid. For this purpose I applied the following formula, the grid is completely buried in the upper layer, without rods in a non-uniform soil [6].

$$R_g = \frac{\rho_1}{\pi L_c} \left[ K_r \left( \ln \frac{2L_c}{a'} + N - 1 \right) + K_1 K_p \left( \frac{L}{\sqrt{A}} - \frac{2(x+1)}{\sqrt{A}} \right) \right] \quad (15)$$

The value that was calculated is of  $21,56\Omega$ .

### 5.3 Test 1 : Fall of potential Method with angled leads

The first test was carried out by using the Fall of Potential method with angled leads at 90 degree. In this case the magnetic flux does not concatenate the potential leads, therefore there is not any presence of AC mutual coupling and the measurements provide the real apparent resistance of the grid.

Test characteristics :

Height o leads above the surface soil	Laying on the ground
Position probe P	100 m
Position probe C	62 m
Length current probe	0.52 m
Length potential probe	0.52 m
Current	2 mA for 52 Hz
Frequency analyzed	52 Hz to 10kHz

*Table 3 Characteristics of the test*

Equipments used as follows :

- Differential probe Chauvin Armoux DP-25
- Current probe Lilco Ct
- Isolating transformer BBM windings LTD
- IMS

The frequency was analyzed varies from 52 Hz to 10 kHz, evaluating the apparent resistance and comparing the measurements by the relative error, by means of the measurements as standard, as shown in th figure 32 and 33 respectively , while the figure 34 shows the real part and imaginary impendence of the grid.

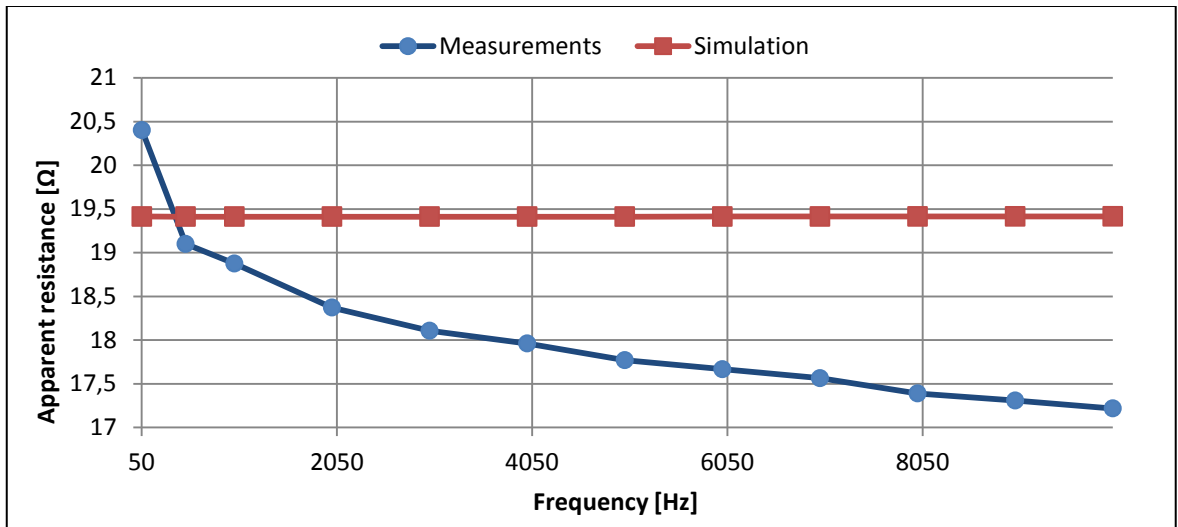


Figura 32 Apparent resistance measurement and simulation with angled leads

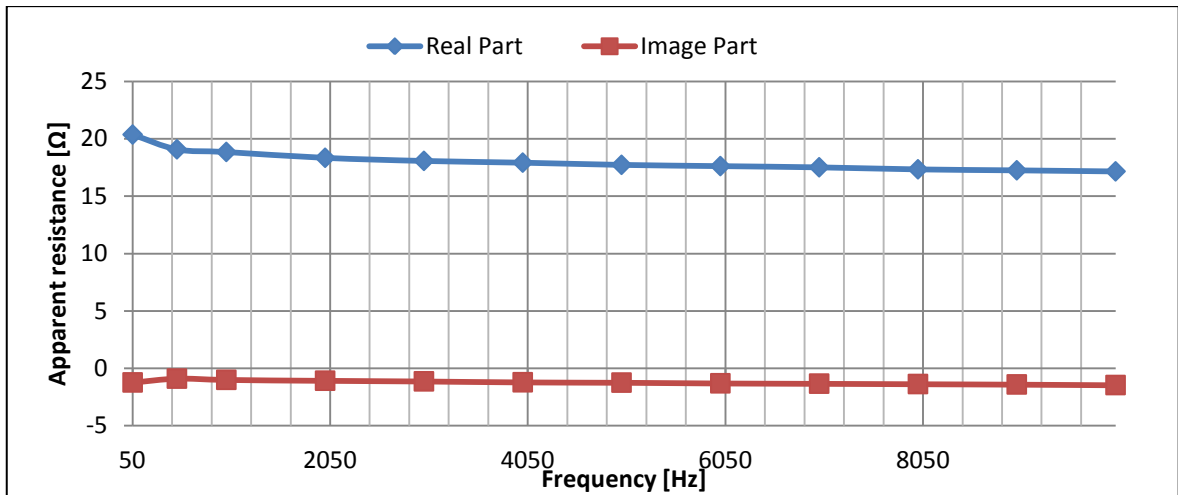


Figura 33 Real part and Image part of the grid

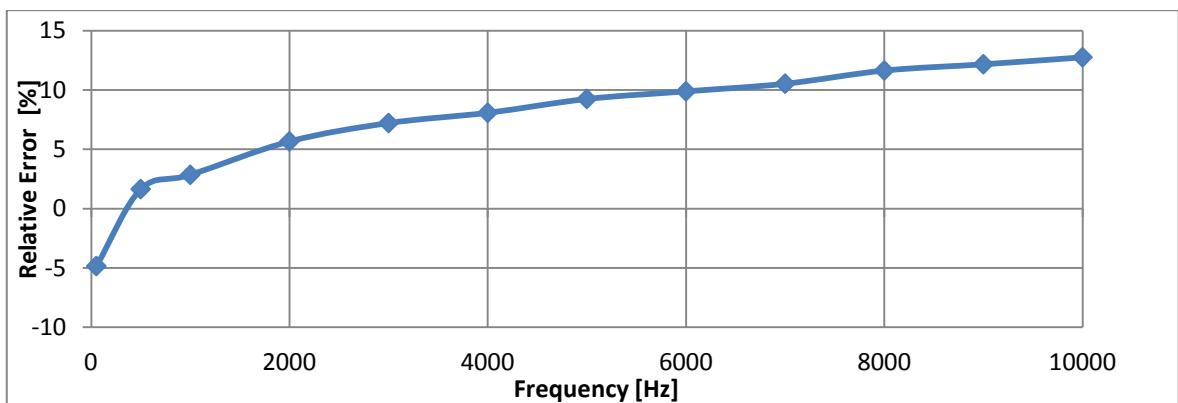


Figura 34 Relative error between simulation and measurements

From the measurements it is possible to note how the grid behaviour is almost completely resistive. The apparent resistance was obtained from measurements have a decreasing trend while by simulation it has is about constant. This difference is probably due to the simulation that does not take into account the real soil behaviour together with changing of frequency. Indeed at increasing of the frequency the conductive soil is as shown in figure 35. It increases and therefore there is a decrease of the apparent resistance of the grid. The maximum relative error is of 10% and it at frequency of 52 Hz .

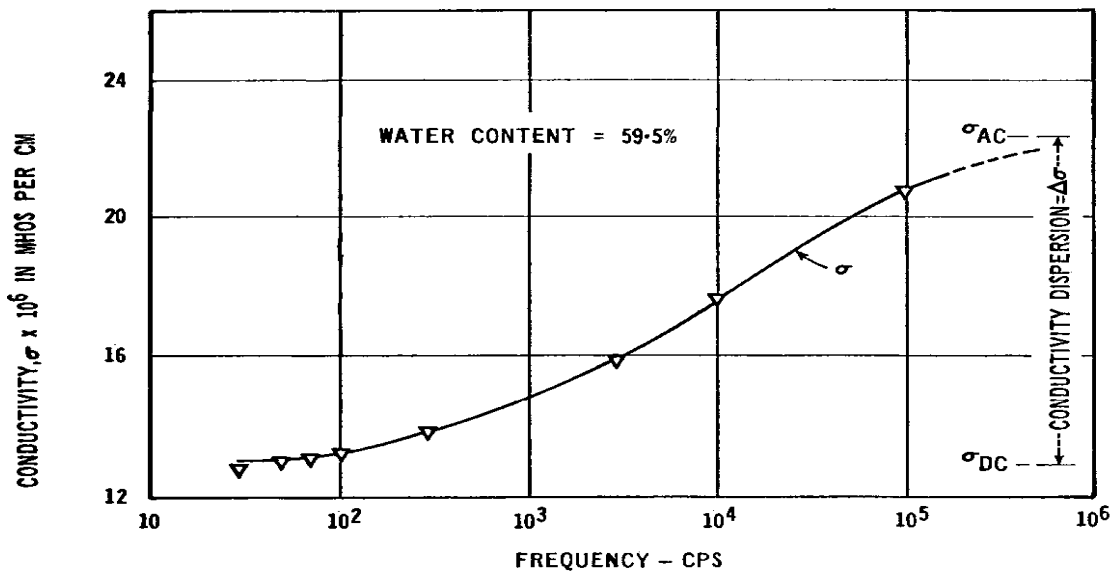


Figure 35 Conductivity increases (resistivity reduces) with frequency ( Reproduced from [15])

#### 5.4 Test 2 : Fall of potential Method with parallel leads, separation 1 m

The figure 36 shows the set up for the second test

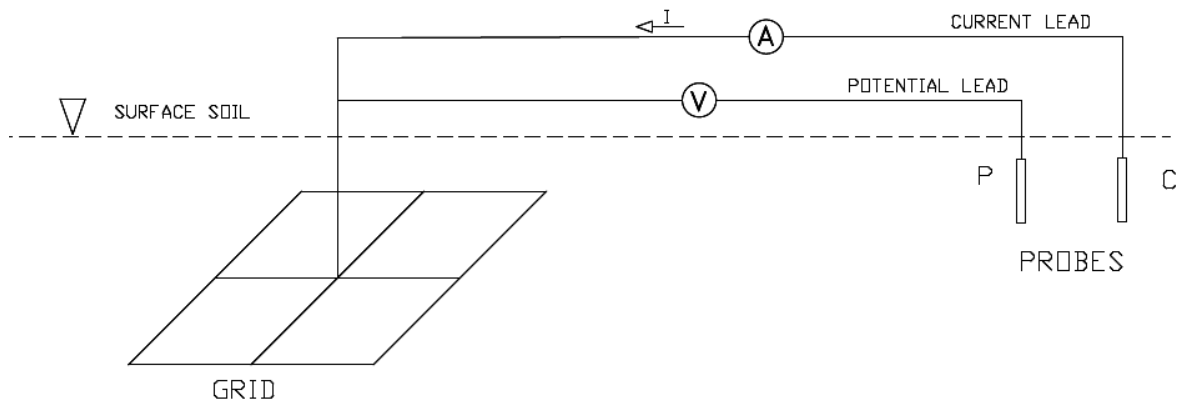


Figure 36 Fall of potential set-up with parallel leads

Test characteristics :

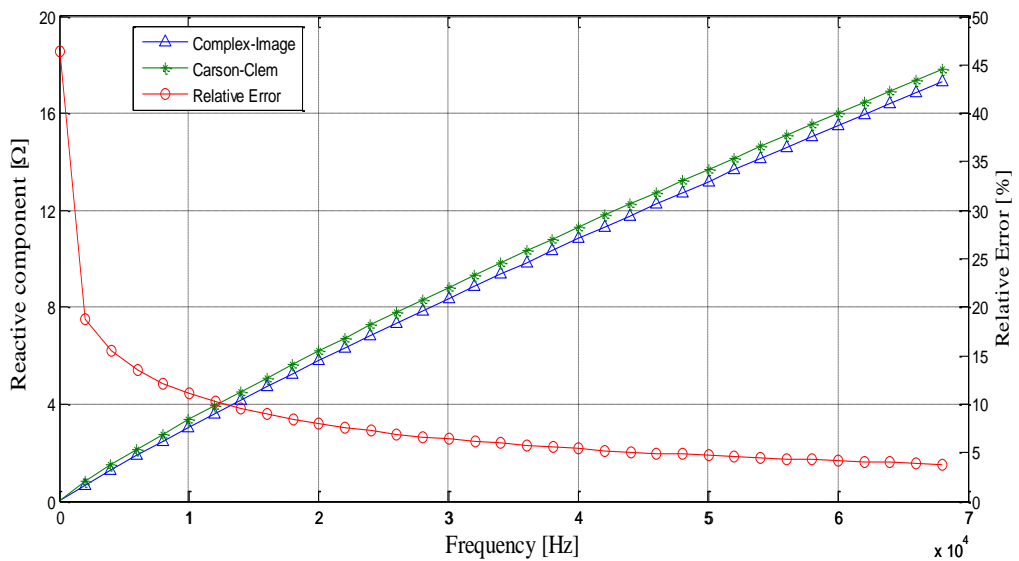
Height leads above the surface soil	Laying on the ground
Position probe P	100 m
Position probe C	62 m
Length current probe	0.52 m
Length potential probe	0.52 m
Current	2 mA for 52 Hz
Frequency analyzed	52 Hz to 70kHz

Table 4 Characteristics of the test

Equipments used as follows:

- Differential probe Chauvin Armoux DP-25
- Current probe Lilco Ct
- Isolating transformer BBM windings LTD
- IMS

In the figure 37-a and 37-b it is estimated the resistive and reactive component of the ac mutual coupling between leads considering the characteristic of the test with Carson-Clem formula and Complex-image formula and the relative error using Carson-Clem as standard.



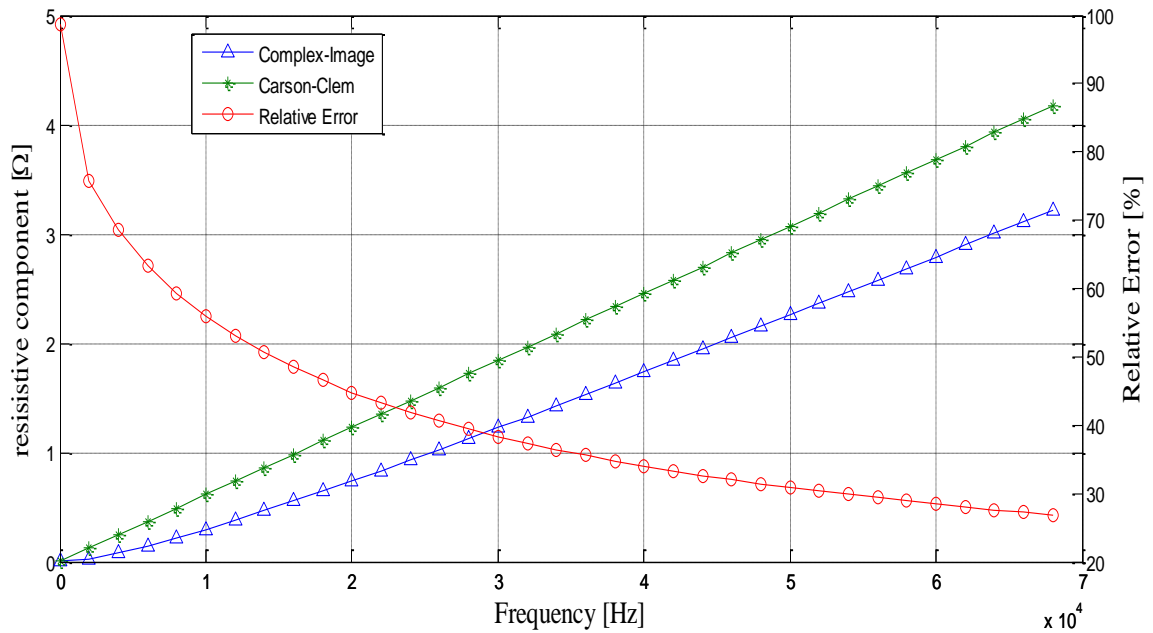


Figure 37-a, 37-b Reactive and resistive component of the ac mutual coupling with parallel leads

We can see how the relative error is high, around 20% for low frequencies and it decreases with increasing of the frequency.

The figure 38 shows the simulated fall of potential method with a separation of 1 m between the current and potential conductor with an operating frequency of 52 Hz. It is evident how there is a huge plateau region. It indicates how the a.c. mutual coupling is negligible to obtain the ground impedance value.

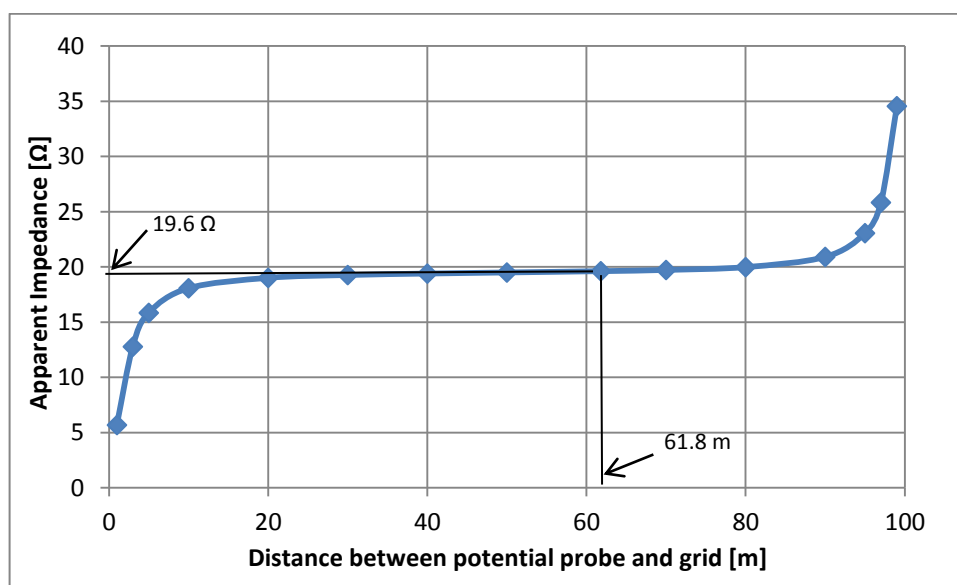


Figure 38 Simulated Fall of Potential measurements

The figure 39 shows the apparent resistance of the grid obtained from measurements and by simulation.

The apparent resistance that was obtained from measurements has a decreasing trend while it is about constant by simulation for frequency from 52 Hz to 10 kHz. This difference is due probably to the simulation that does not take into account the real soil behaviour together with changing of frequency. In fact at increasing of the frequency the conductive soil increases and therefore there is a decrease of the apparent resistance of the grid. After 10 kHz the apparent resistance starts to rise because the a.c. mutual coupling increases together with the frequency, with a similar trend for both. Despite these differences the measurements and simulation trends are similar.

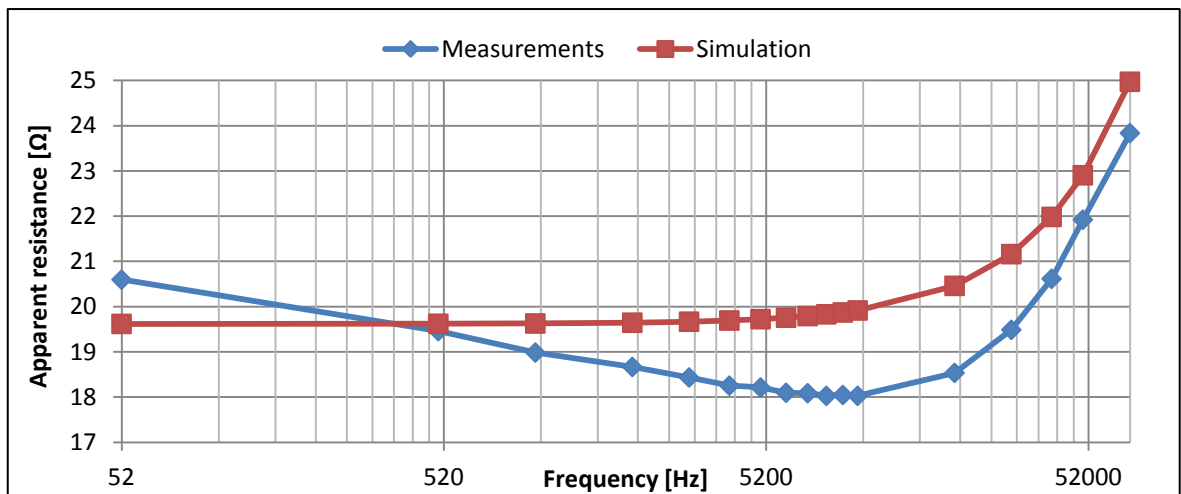


Figure 39 Apparent resistance measurement and simulation with parallel leads

The figure 40 shows the apparent resistance angle of the grid obtained from measurements and by simulation. For both the trend is similar in all the interval analyzed still with some differences .

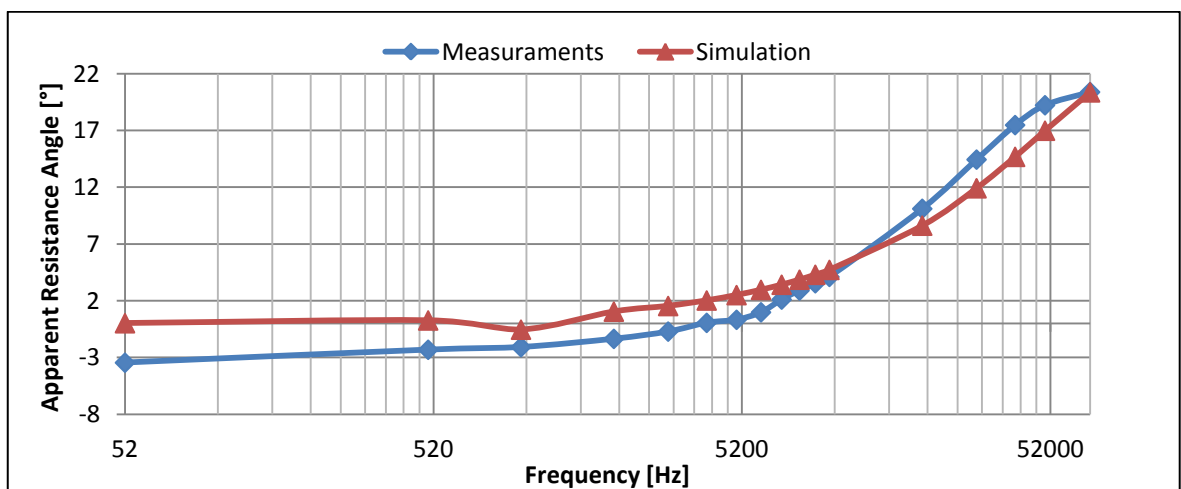


Figure 40 Apparent resistance angle measurement and simulation with parallel leads

The figure 41 shows the relative error between measurements and simulation with the measurements as standard. The maximum relative error is of about 10 % for the lowest frequency of 52 Hz .

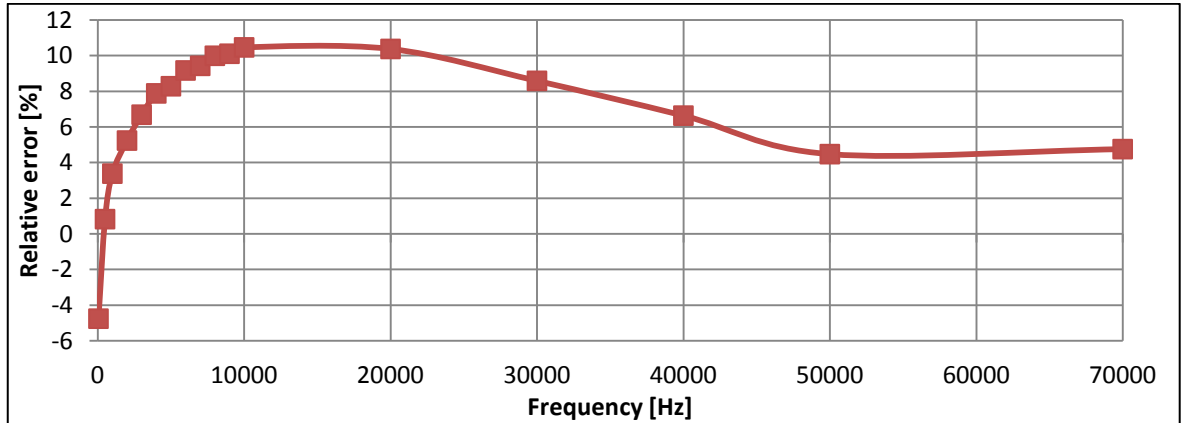


Figure 41 Relative error between simulation and measurements

The figure 42 shows the apparent resistance of the grid obtained from measurements considering or not the ac mutual coupling. The red line represents the real apparent resistance, so without the mutual coupling calculated by Carson-Clem formula. It has values lower than the one obtained with ac mutual coupling especially for high frequency where the concatenated flux is important. However for these frequencies the apparent resistance has not a constant trend probably due to the inductance of the conductor.

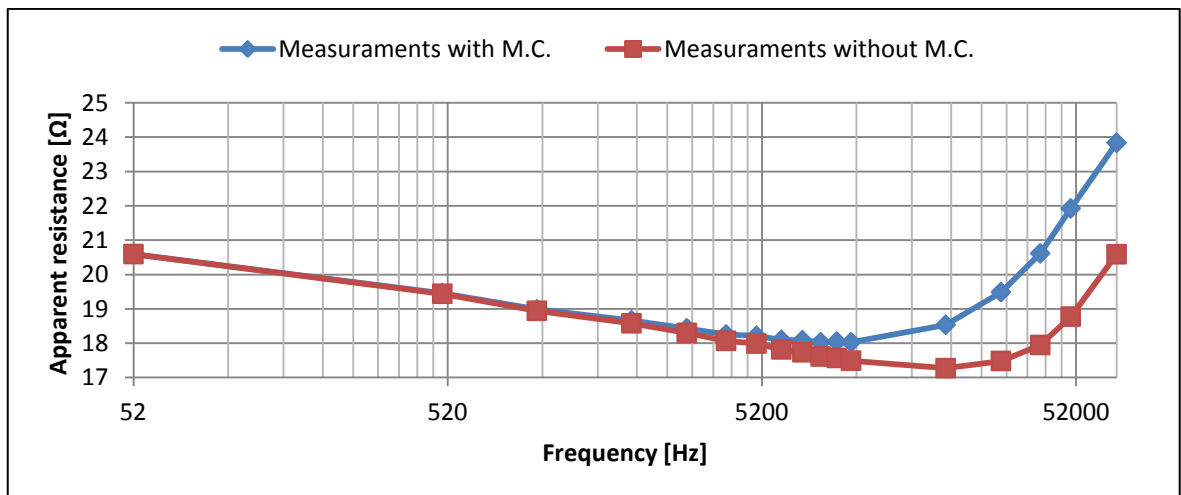


Figure 42 Apparent resistance measurements with and without ac mutual coupling



Equally way the figure 43 shows the apparent resistance of the grid obtained by simulation considering or not the ac mutual coupling calculated by using Image formula. We can take into account the same preceding evaluations, considering the soil conductivity.

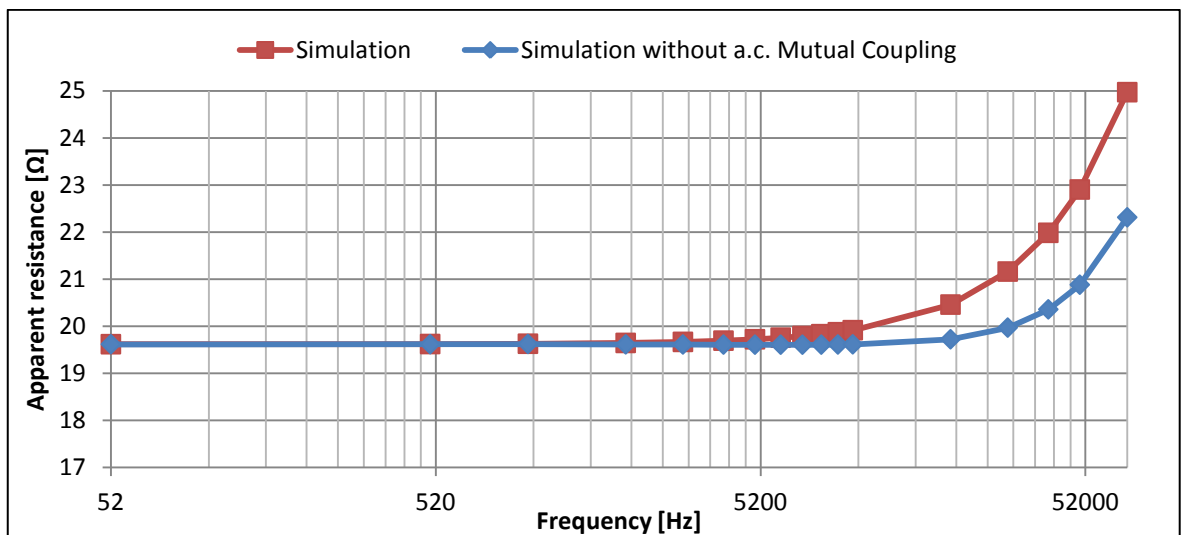


Figure 43 Apparent resistance simulation with and without ac mutual coupling

### 5.5 Test 3 : Fall of potential Method with parallel leads, separation about 0,06 m

The third test was based on the same set up of the second one but in this case the leads are very close, the separation is about 6 cm.

Characteristics test :

Height leads above the surface soil	Laying on the ground
Position probe P	100 m
Position probe C	62 m
Length current probe	0.52 m
Length potential probe	0.52 m
Current	2 mA for 52 Hz
Frequency analyzed	52 Hz to 70kHz

Table 5 Characteristics of the test

Equipments used as follows:

- Differential probe Chauvin Armoux DP-25
- Current probe Lilco Ct
- Isolating transformer BBM windings LTD
- IMS

In the figures 44-a and 44-b were estimated the resistive and reactive component of the ac mutual coupling between leads considering the characteristic of the test with Carson-Clem formula and Image formula and the relative error, it using the Carson-Clem as standard.

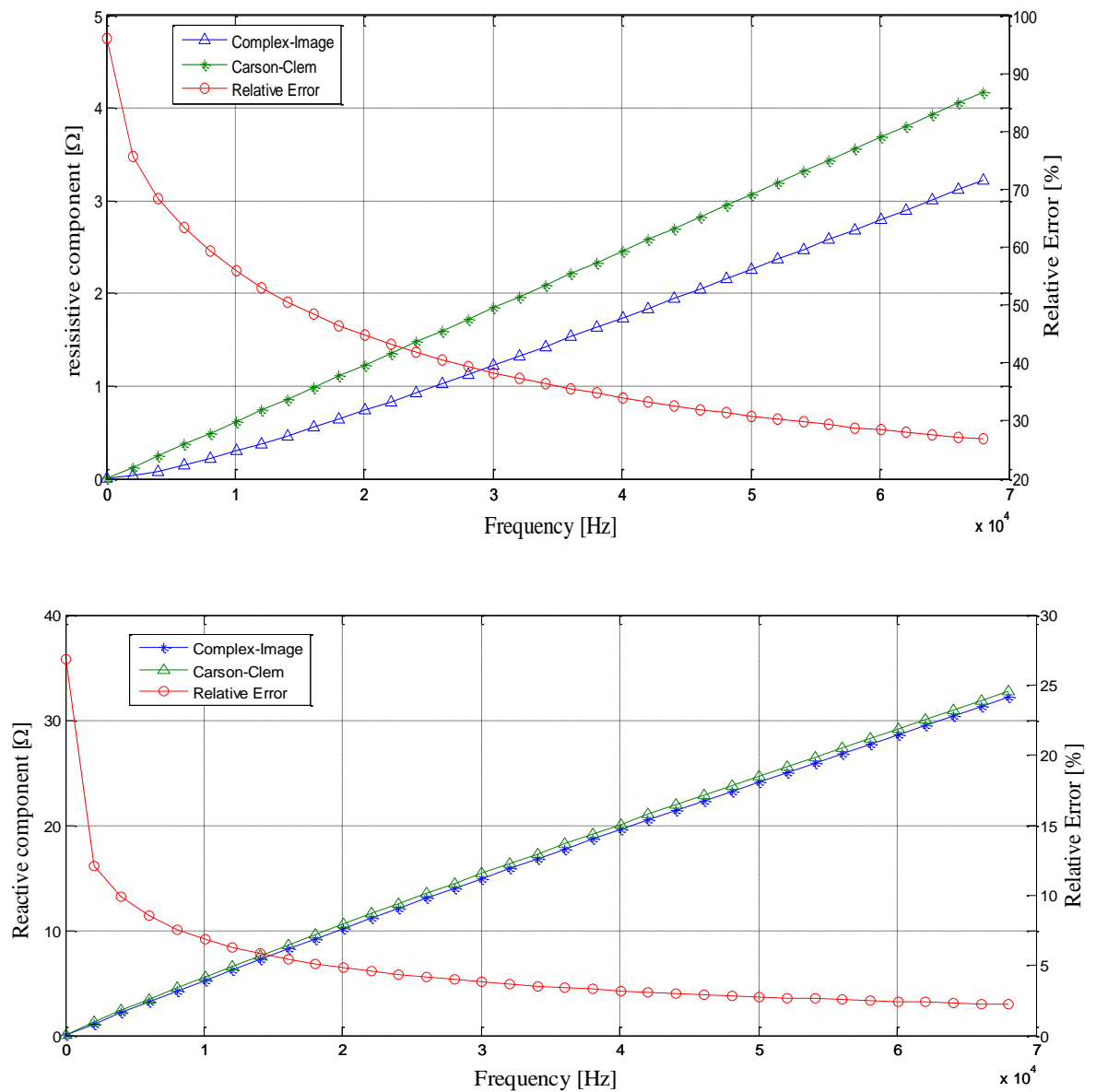


Figure 44-a, 34-b Reactive and resistive component of the ac mutual coupling with parallel leads

The figure 45 shows the apparent resistance of the grid obtained from measurements and by simulation. Even if it is not so evident there is a slight effect of the soil conductivity for the first frequencies, it is lower than the one obtained with a separation of 1 m because the ac mutual coupling is more substantial . After the 10 kHz the apparent resistance starts to rise because the a.c. mutual coupling increases with the frequency with a similar trend for both.

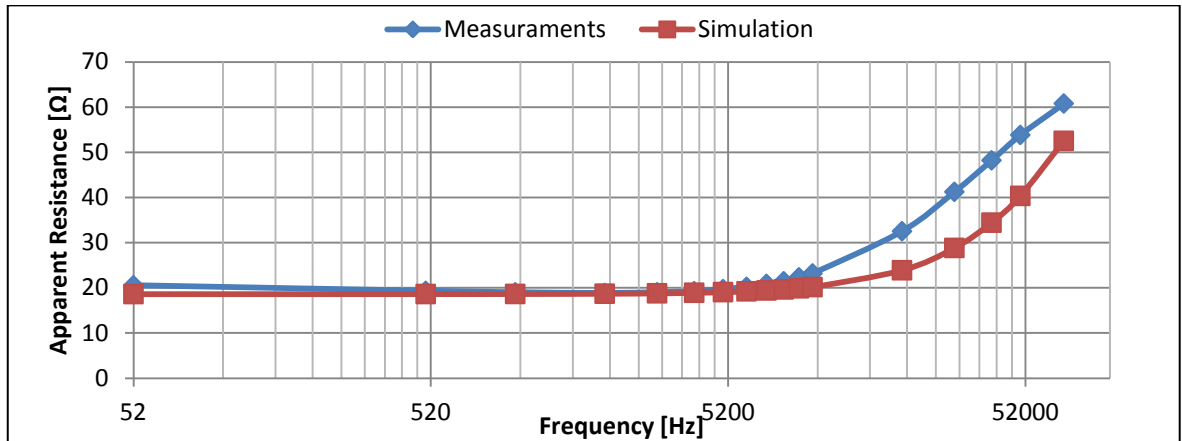


Figure 45 Apparent resistance measurements and simulation with parallel leads

The figure 46 shows the apparent resistance angle of the grid obtained from measurements and by simulation. For both the trend is similar for all the interval analyzed still with some differences .

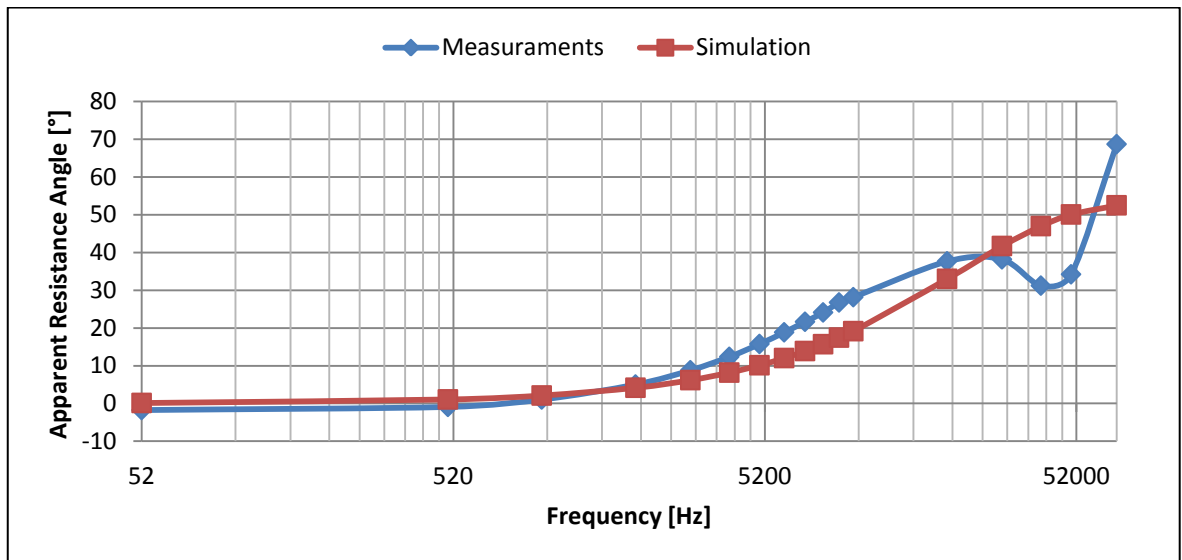


Figure 46 Apparent resistance angle measurement and simulation with parallel leads

The figure 47 shows the relative error between measurements and simulation with the measurements as standard. The maximum relative error is of about 30% for the frequency of 30 kHz

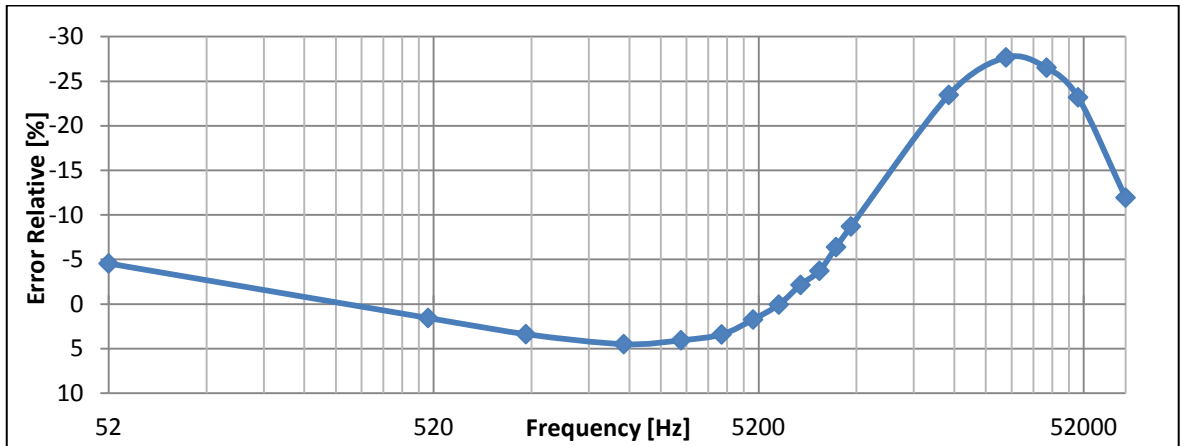


Figure 47 Relative error between simulation and measurements

The figure 48 shows the apparent resistance of the grid obtained from measurements considering or not the ac mutual coupling. The red line represents the real apparent resistance, so without the mutual coupling calculated by Carson-Clem formula. It has values lower than the ones obtained with ac mutual coupling especially for high frequency whereas the concatenated flux is important. However for these frequencies the apparent resistance has not a constant trend probably due to the inductance of the conductor.

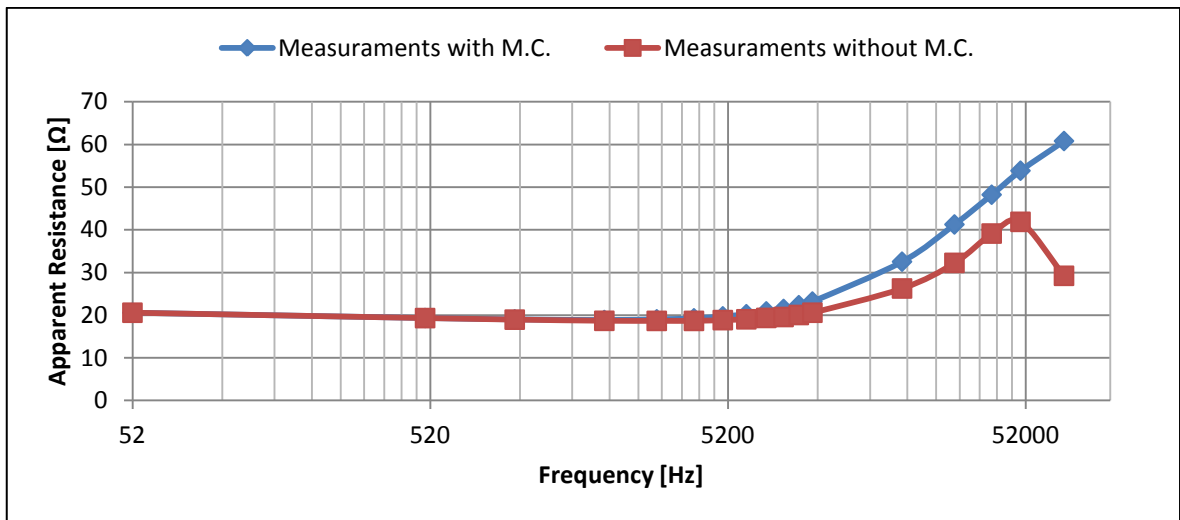


Figure 48 Apparent resistance measurements with and without ac mutual coupling

Equally the figure 49 shows the apparent resistance of the grid obtained by simulation considering or not the ac mutual coupling calculated by using Carson-Clem formula. The values obtained without the ac mutual coupling are still lower than the ones obtained with ac mutual coupling especially for high frequency where the concatenated flux is important. However for these frequencies the apparent resistance (without ac mutual coupling) has not a constant trend probably due to the inductance of the conductor.

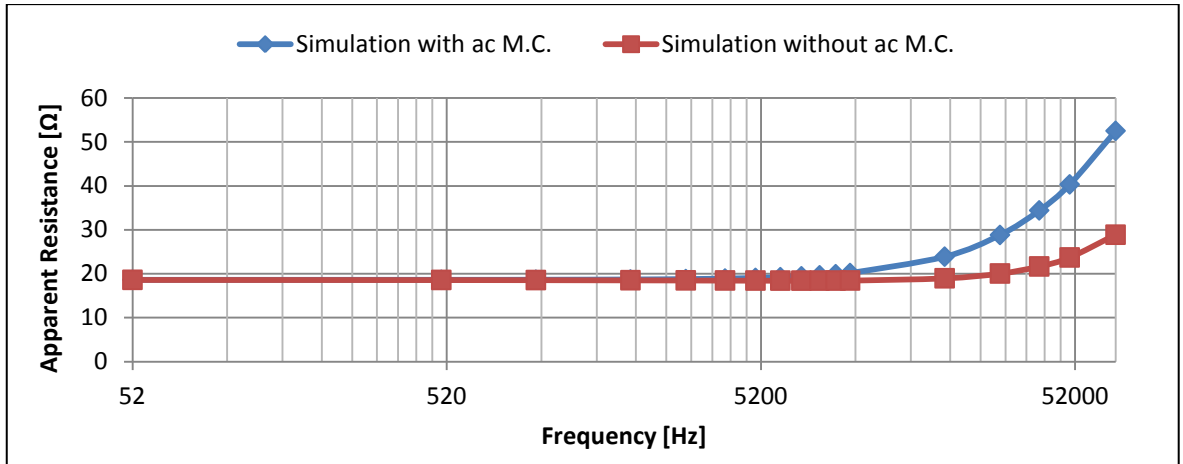


Figure 49 Apparent resistance simulation with and without ac mutual coupling

As the figures 50-a and 50-b show there is an interesting comparison between the calculation of the mutual coupling by the Carson-Clem formula and by the apparent resistance values obtained from the test 1, therefore with leads angled, and the test with parallel leads with a separation of 1 m and 0,06 m for the measurements and simulation.

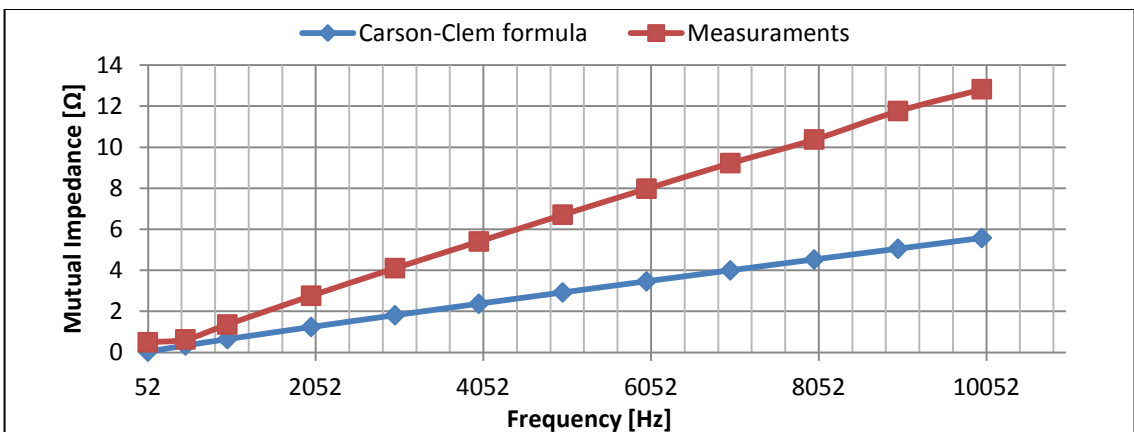
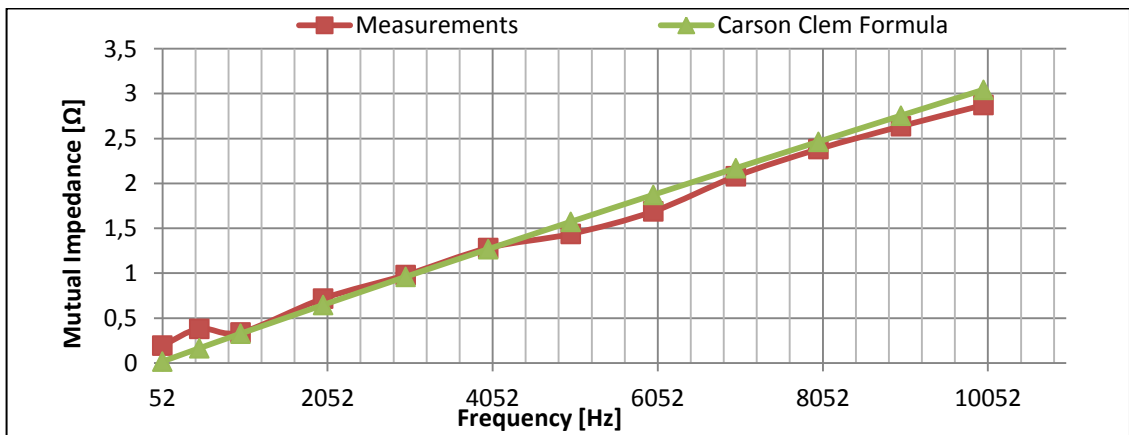


Figure 50-a, 50-b Comparison for the calculation of the mutual coupling

It is possible to note how for the separation of 1 m the mutual coupling calculated has similar trend for all the interval and the one obtained from measurements and by analytical

calculation is really close. Indeed with separation of 0.06 m we still have a similar trends, although the values are not so close.

## 5.6 Conclusions

After so many measurements and implementations it is important to sum up the main results and their differences, trying to figure out the reasons. The range of analyzed frequencies is from 52 Hz for having a value of apparent impedance of the grid free from errors caused by noise at 50 Hz, up to 70 kHz for enhancing the ac mutual coupling between current and potential conductor. Indeed, since the grid analyzed of relatively small dimensions and therefore of high earth impedance, with using of short conductors for the achievement of the remote earth the exaltation of this magnetic phenomenon is viewable at very high frequencies only. In the first test with angled leads we have seen how there is a important difference between measurements and simulation trends, indeed the simulation seems to do not to take into account the phenomenon of the real soil behaviour with the chancing of the frequency. At the increasing of the frequency the conductive soil increases and therefore there is a decrease of the grid's apparent resistance. This causes obviously repercussions in the other tests in a more or less evidence depending on the value of the mutual coupling and on the distance between leads. In all tests with low frequencies, 52 Hz, a value of apparent resistance has been found greater t for the measurements than with the simulation. This difference is not due to mutual coupling being negligible, but probably to a choice of the terrain model that represents the real behaviour of the ground or to a precise representation of the grid that does not have a precise plan. The measurements of the soil resistivity were carried out in several previous years and its value may be changed due to seasonal variations. However, the relative error obtained between simulation and measurements is estimated at around 10% which is more than acceptable. After this initial analysis it was decided to calculate and apply the Complex-image formula for calculating the mutual coupling on the second and third tests. The results showed lower values of ground impedance for high frequencies but above all at a constant impedance to ground, probably due to the inductive component of the conductor that appears both in simulations and in measurements. Then a comparative evaluation of measures formula has been made in the calculation of the mutual coupling for frequencies from 52 Hz to 10 kHz . The results show some very interesting peculiarities. In the first case, the Carson-Clem formula has presents similarities with more measurements while in the second one there are have still a similar trends, however the values are not so close. These last results seem to indicate that the analytical evaluation of the mutual coupling does not lead to satisfactory results when the conductors are close. More measurements should be performed in order to identify whether there is a distance beyond which the complex-image formula is not applicable. These tests confirm the need of an assessment by means of direct measurements of any ground system in high frequency, especially for installations of large earthing systems.

## 6 Fall of potential method with coaxial cable

### 6.1 Introduction

The second part of the tests has been carried out is based on the fall of potential method but with a variation idealized by Prof. Huw Griffiths. As shown in the figure 51 the method uses a single coaxial cable to analyze the earth impedance for grounding systems, the core of the coaxial cable is used for flowing the current between the grid and the current probe C, while the screen of the conductor is used for evaluating the voltage between the grid and the potential probe P. As we all know, the current passing through the core is creating a mutual coupling between it and the screen of the coaxial cable, causing an incorrect evaluation of the potential tension between the grid and probe P. This new method has been applied and analyzed in two different steps, an analysis in the laboratory for trying to understand and evaluate what was the behaviour of this method and an analysis on the same grid where I had previously applied the fall of potential method.

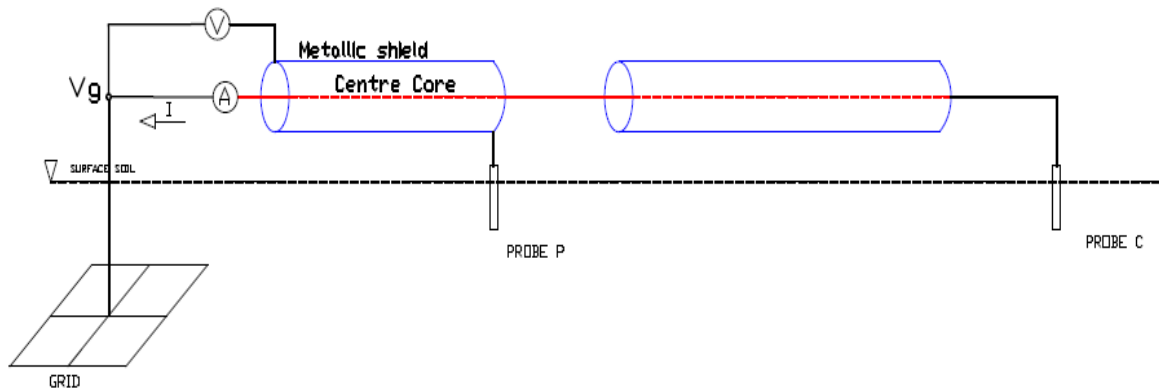


Figure 51 Fall of potential method with coaxial cable set-up

## 6.2 Laboratory

In the laboratory the analysis was based on the circuit diagram shown in the figure 52. The purpose was to evaluate the mutual coupling behaviour and the coaxial cable has come to be used on the field tests.

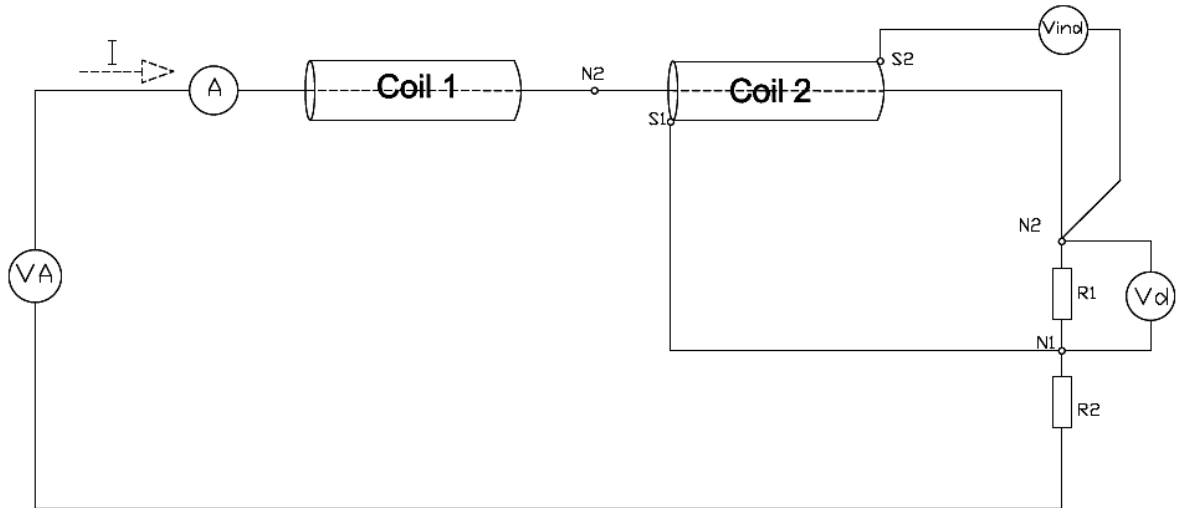


Figure 52 Electric circuit analyzed in laboratory

To evaluate the mutual coupling between shield and core of the coil 2 it was decided to compare two measurements, the first one referred as the direct voltage and indicated by  $V_d$  (it is the voltage across the resistor  $R_1$  with no mutual coupling created by coil 2). The second one is the indirect voltage and indicated by  $V_{ind}$  (it is still the voltage across the resistor  $R_1$  but in it is used the shield of the coil 2 is used. The difference of the two measurements should allow to evaluate the voltage induced on the shield of the coil 2.

A first evaluation of the electric circuit was performed by using the following equipment:

- Differential probe Chauvin Armoux DP-25
- Current probe Lilco Ct
- Voltage regulator Hossoni SV-4°
- Lecroy wave runner 64 Xi oscilloscope



The main features of the coils are summed up in the table 6

	Length [m]	Resistance [ $\Omega$ ] (measured by multimeter)	radius internal [mm]	radius external [mm]
Coil 1	69.4	2.80	: 0,5	2,8
Coil 2	108.75	4.41	2,8	2,8

Table 6 Main characteristics of the coaxial cables

As shown in the figure 53 the voltage induced was evaluated as a function of the current for two different set up, changing the values of R1 and R2 and the supply voltage is provided the electricity network and its value is varied by a voltage regulator. The first one with spooled coils and the second one with coils lying on the ground floor of the laboratory.

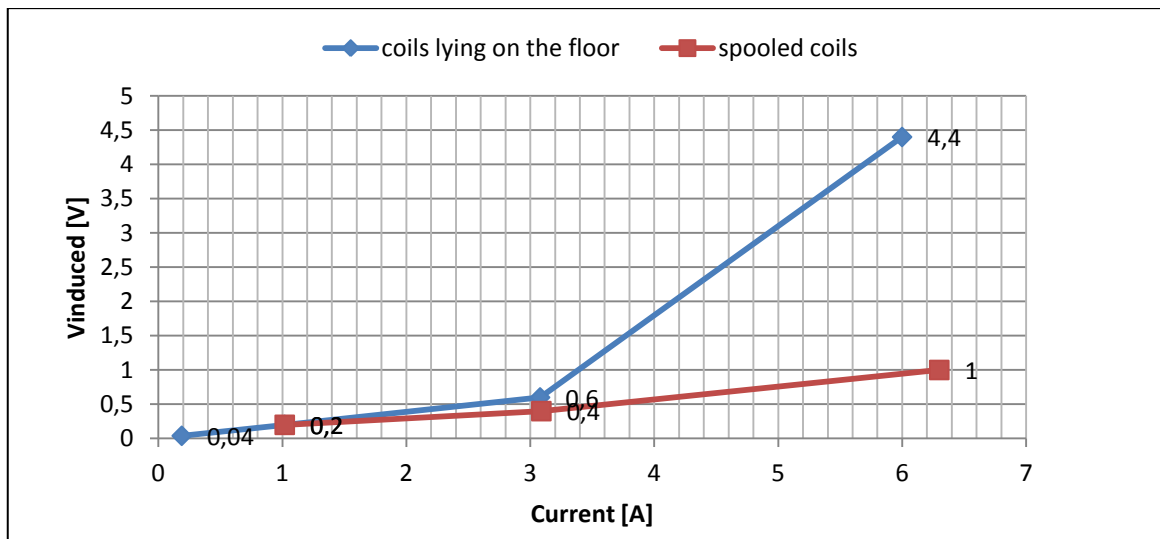


Figure 53 Voltage induced as fuction of the current for two different set-up

Although the current values for both set-up are not exactly the same as you can see, in the second one the induced voltage for high current values, about 6 on the amp, is significantly lower. This phenomenon should be due to the higher flow concatenated with spooled coils, that results in a higher induced voltage.

After several problems due to a non-operation of all circuit connections, the presence of distorted waveforms and the need of using high values of current and have a regulation more accurate of the different parameters, it was decided to analyze the circuit as a function always of the current but also the frequency by means a different device for supplying the voltage at the circuit.

The equipment used as follows :

- Differential probe Chauvin Armoux DP-25
- Current probe Lilco Ct
- Isolating transformer BBM windings LTD
- IMS
- Lecroy wave runner 64 Xi oscilloscope

It was decided to assess the dependence of the induced voltage in the range of R2, using a very low value of R1. The figure 54 shows the voltage induced as a function on of the current for a constant value of  $R1 = 0.6 \Omega$  while R2 changes.

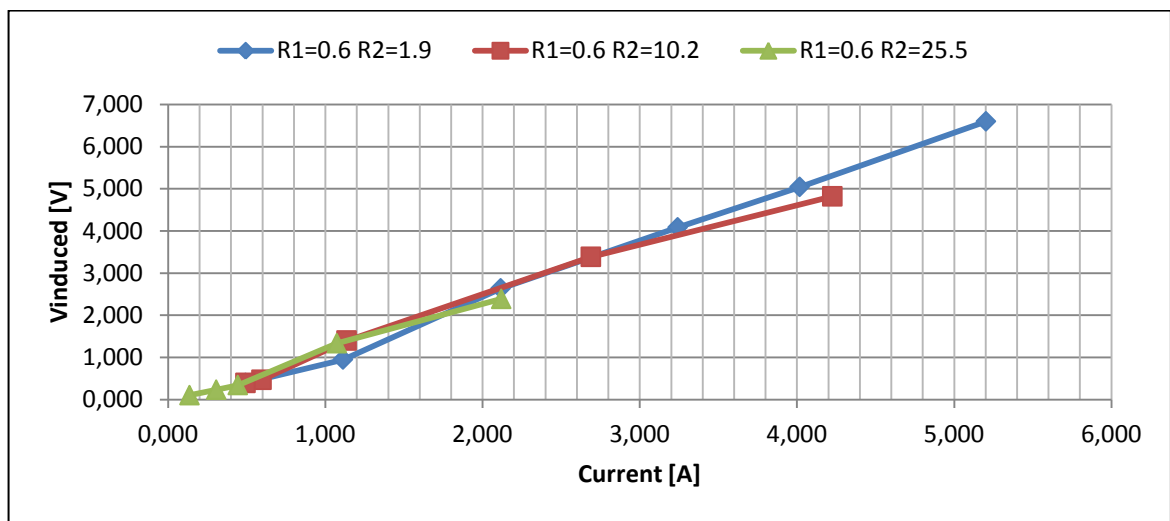


Figure 54 : voltage induced as function on the current for a constant value of R1 while R2 changes

The voltage induced trend is pretty linear for every kind of measurement. This confirms the independence of the mutual coupling from the value of R2 and a linear dependence from the current.

The induced voltage was assessed as a function of frequency. This evaluation was carried out following the field tests since an analysis in the frequency was not previously planned.

Characteristics of the circuit are listed in the table 7

R1	20 $\Omega$	Measured by multimeter
R2	229,8 $\Omega$	Measured by multimeter
Length coil 1	40 m	Approximate value
Length coil 2	70 m	Approximate value
Resistance coil 1	1,7 $\Omega$	Measured by multimeter
Resistance coil 2	2,8 $\Omega$	Measured by multimeter

Table 7 Characteristics of the circuit

The figure 55 shows the voltage induced as a function of frequency from 52 Hz to 70 kHz for both set-up. The two tests were performed with a current value very similar to each other, figure 56, except for frequencies from 20 kHz to 50 kHz where the behaviour of resistor R1 will behave differently, figure 57.

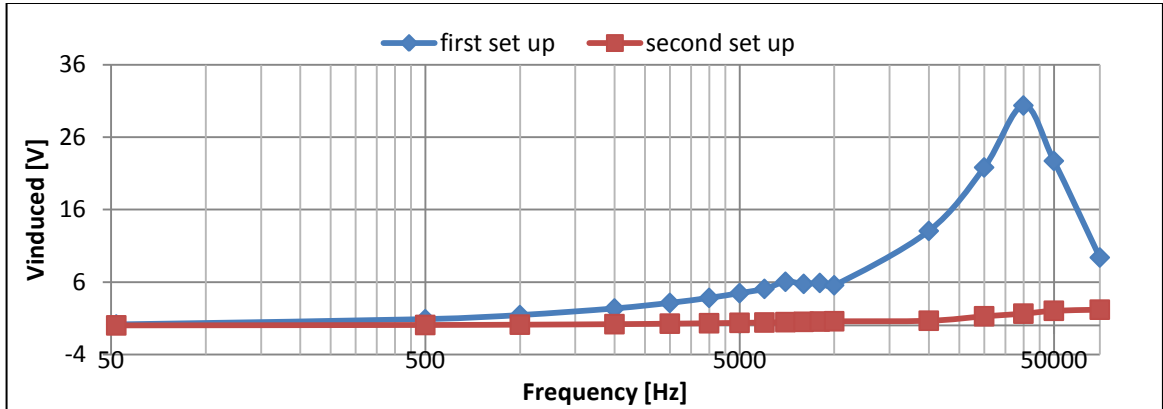


Figure 55 Voltage induced as function for the two set-up

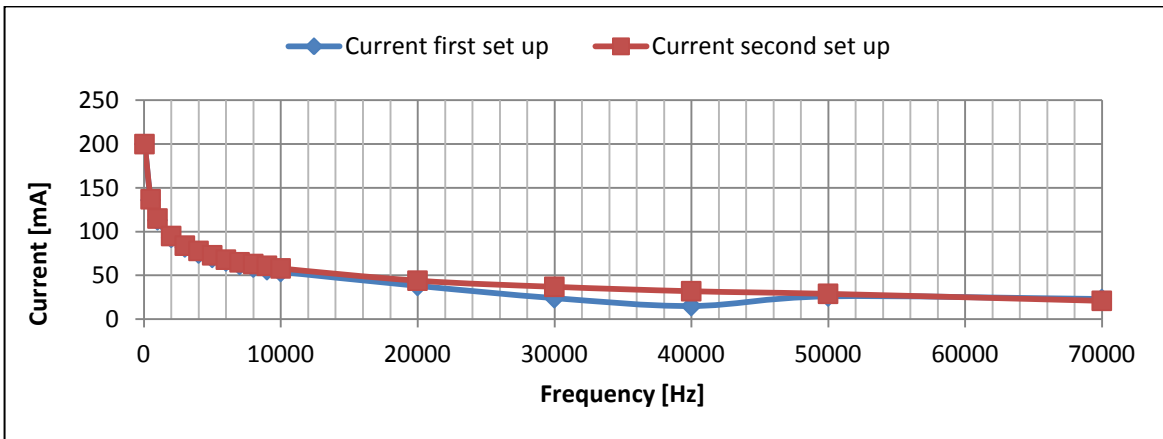


Figure 56 Current flowing in the two set-up

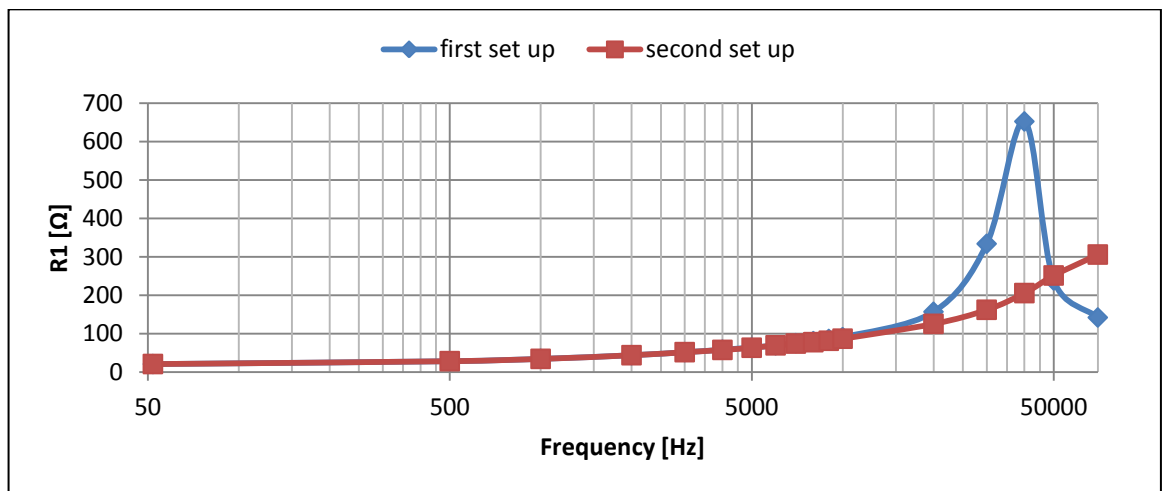


Figure 57 Module of R1

The analysis was performed on resistors which have not purely resistive behavior as the frequency increases, inductive and capacitive components influence the module of the resistor creating possible resonance phenomena as shown in Figure 57. The two set-up differ especially for the induced voltage, in the first case where I have larger values, confirming the increased flow concatenated with coils wound. The induced voltage has a different trend depending on the set-up but both are similar to those of the resistance R1 of the same, similarity that it requires a further investigation. The first test seems to present a phenomenon of resonance by the resistor R1 which is not the second one although the frequencies analyzed are the same. This difference appears to be due only by the arrangement of the coils.

### 6.3 Field tests

After an analysis in the laboratory the coaxial cable was used for evaluating the grid at Llanrumney, Cardiff (UK). The frequencies that were analyzed here are just a few, so it is not feasible a precise comparison with the others results obtained for the same grid.

The equipment used follows :

- Differential probe Chauvin Armoux DP-25
- Current probe Lilco Ct
- Isolating transformer BBM windings LTD
- IMS
- Lecroy wave runner 64 Xi oscilloscope

Characteristics test are summed up in the following table :

Height lead above the surface soil	Laying on the ground
Position probe P	100 m
Position probe C	62 m
Lenght current probe	0.52 m
Lenght potential probe	0.52 m
Current	2 mA
Frequency analyzed	52 Hz, 500 Hz, 20 kHz, 70 kHz

*Table 8 Characteristics of the test*

The figure 58 shows the apparent resistance for four different frequencies, while the table 9 sums up the values of the apparent resistance for the grid, that was analyzed showing its resistive and reactive component, for the classic fall of potential method with separation 1 m and 6 cm, and with the fall of potential method with coaxial cable.

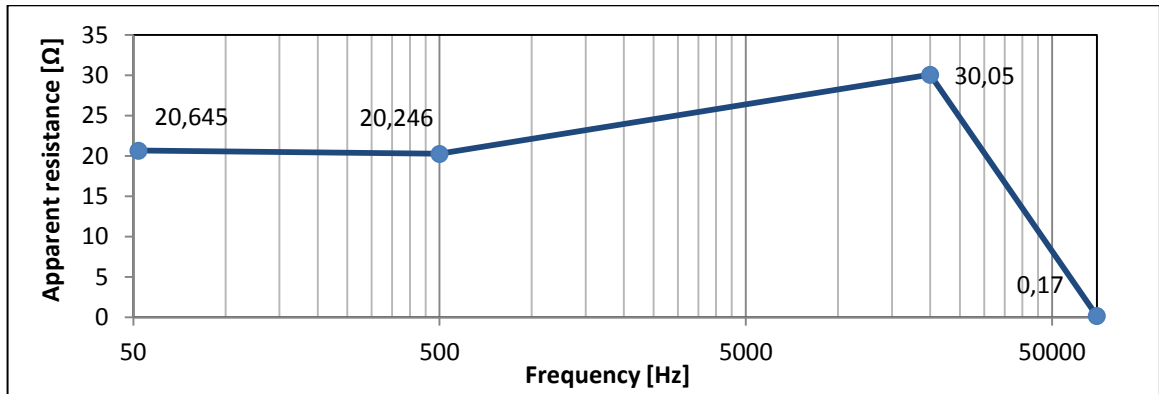


Figure 58 Apparent resistance by using the fall of potential method with coaxial cable

Frequency	1 m			6 cm			Coaxial cable		
	r [Ω]	x [Ω]	z [Ω]	r [Ω]	x [Ω]	z [Ω]	r [Ω]	x [Ω]	z [Ω]
52 Hz	20,56	-1,23	20,56	20,483	-1,713	20,559	20,635	-0,67	20,64
500 Hz	19,44	-0,78	19,459	19,321	-0,314	19,323	19,735	4,510	20,24
20 kHz	18,428	3,254	18,535	25,751	19,86	28,51	22,059	22,406	31,44
70 kHz	22,343	8,305	23,836	22,102	56,629	60,789	0,169	0,0087	0,169

Table 9 Apparent resistance by using the fall of potential method and the version with coaxial cable

To evaluate the mutual coupling between the core and the shield it has been used the following formula taking as earth resistivity of 130 Ω·m. It is the Carson-Clem formula readapted for coaxial cable [10] :

$$Z_{ij} = Z_{ji} = \left( \pi^2 \cdot 10^{-4} \cdot f + j4\pi \cdot f \cdot 10^{-4} \ln \frac{D_e}{d_{ij}} \right) [\Omega/km] \quad (16)$$

Where :

$$D_e = 659 \sqrt{\frac{\rho}{f}} \text{ equivalent depth of hypothetical return path of the earth current}$$

$d_{ij}$  = mutual distance [m] between conductors  $i$  and  $j$ , when the conductors  $i$  and  $j$  are coaxial ones, it yields  $x_{ij} \approx x_{ji} = x_{ji}$  where  $j$  is the external conductor and  $i$  the inner one, see figure 59.



Figure 59 configuration with coaxial cables

The values that are sum up in the table for the frequencies was been analyzed. From the difference between the measurements and mutual coupling impedance is possible to find the real apparent resistance behaviour without the influence of the mutual coupling, as shown in table 10.

	r [ $\Omega$ ]	x [ $\Omega$ ]
f= 52 Hz	0,0032	0,052
f= 500 Hz	0,0307	0,4556
f = 20 kHz	1,2276	15,3499
f = 70 kHz	4,2966	50,3086

Table 10 Mutual coupling calculated by Carson-Clem formula

	1 m			6 cm			Coaxial cable		
Frequency	r [ $\Omega$ ]	x [ $\Omega$ ]	z [ $\Omega$ ]	r [ $\Omega$ ]	x [ $\Omega$ ]	z [ $\Omega$ ]	r [ $\Omega$ ]	x [ $\Omega$ ]	z [ $\Omega$ ]
52 Hz	20,56	-1,21	20,59	20,47	-1,75	20,55	20,632	-0,15	20,63
500 Hz	19,44	-0,55	19,41	19,29	-0,64	19,30	19,704	4,05	20,12
20 kHz	17,02	-2,91	17,27	24,52	9,31	26,23	20,835	5,056	21,43
70 kHz	18,06	9,886	21,212	17,819	23,143	29,2	-4,11	-50,45	50,45

Table 11 Apparent resistance without mutual coupling

Although the analyzed frequencies are unfortunately a few considerations can be made. Looking at the data you may notice a reactive component coax more than the other tests as shown in table 11, it is due to the extreme proximity of the core and the screen. However, for 70 kHz, the apparent resistance its component decreases totally, phenomenon that I have not found evidence in the literature.

With angled leads were obtained the following values for the apparent resistance:

$$f = 52 \text{ Hz } \dot{Z}_g = 20,364 - 1,2348i \text{ } [\Omega]$$

$$f = 500 \text{ Hz } \dot{Z}_g = 19,071 - 0,897 \text{ } [\Omega]$$

Applying Carson-Clem formula for coaxial cables as shown in table 11 results that are obtained from the values obtained with angled leads are rather inconsistent, especially for the reactive component at 500 Hz

This may indicate that the application of the formula for the calculation of the mutual coupling between core and the screen is not fully realistic whereas the analysis made with conductors angled test that allows us to obtain the real behaviour of the grid was not influenced by the mutual couplings current conductor.

The reasons may be many but the ones identified are:

- Carson-Clem formula is based on homogeneous soils
- Phenomena of end-effects may be present and not considered in the results

## **6.4 Conclusions**

The fall of potential method with coaxial cable was analyzed in two main steps, in the lab and on field tests. The first analysis allowed me to highlight some peculiarities of the circuit and to confirm the principles of physical. The analysis was carried out at low frequency by varying some parameters such as R1 and the current. It was then noted a real linear dependence of the induced voltage by the current. Always in the laboratory analysis of the circuit to vary the frequency has led to a resonance phenomena not fully identified. About the field tests, unfortunately synthesize in four different frequencies, so it was not possible to make an accurate comparison with the classic fall of potential method. However the earth impedance of the grid frequency at 50 Hz is very similar to that obtained with conductors angled, this thanks to a low frequency and to a length of the ground conductor relatively short as not to cause a important ac mutual couplings, this has demonstrated applicability for ground systems of relatively small dimensions. For frequencies of 500 Hz and 20 kHz there is a mutual coupling greater than in tests with separation of 1m and 6 cm, due to the extreme proximity between potential and current conductor. This method the advantage of having only one conductor for the analysis of earth impedance. This means a shorter time for the analysis of grounding systems especially large where the remote earth is at a considerable distance. To obtain a more accurate evaluation on the applicability of the medium, further tests should be performed with large grounding systems where the precision of the impedance value of is greatly influenced by the mutual coupling for low frequencies and have no phenomena of end effects that does not allow you to apply correctly the Carson-Clem formula.





## 7 General Conclusions

At the end of the university studies, I spent a period of about four months was conducted at the University of Cardiff (UK) under the supervision of Prof. Huw Griffiths and with the support of Prof. Roberto Turri, the man who allowed me to undertake this experience with the Erasmus Placement. This period s can be divided into three main steps. The first one was employed to acquire all the necessary knowledge concerned with the earthing system parameters and their Influence. The second one can be divided into a part of numerical analysis with the use of the software CDEGS for the evaluation of the ground impedance of an isolated grid located at Llanrumeny by applying the Fall of Potential Method. This software requiring a model that represents the soil resistivity and it forced me to an important choice such as the interpretation of the soil resistivity data. The simulations obtained have proved to be rather similar with the measurements carried out on the same grid showing some discrepancies for very high frequencies and in the case of angled lead with a phenomenon of reduction of the ground impedance as the frequency increases. During the same period I had the opportunity to work in the laboratory for the evaluation of a new method for calculating the ground impedance with coaxial cable. I could then become familiar with various equipment which then would be used during field tests. The purpose was to obtain a greater manual skills and analytical capacity in the electrical measurements. The third step was based on field tests mainly with application of the fall of potential method and a brief analysis on only a few frequencies for the method with coaxial cable. All this was followed by 'data analysis and writing of the thesis. I have been able to confirm the simulations and note a probable inapplicability of Image Formula for calculating mutual coupling of closely conductors. In the brief period I analyzed a small part of the grounding systems but I recognized it most interesting and useful. Such experience, besides the developing of this thesis, has allowed me to improve the personal knowledge that in those concerned with the electric measurements, measurement methodology, and measurement equipments and to see all the problematic that characterize a real field surveying. Moreover, the closeness with a big research group composed by University Teachers, Researchers and Ph.D. students has let me known, how a research team works and how a research work is developed.



## **Acknowledgements**

Some thanks to people who allowed me to make this experience and who supported me before and during it.

Dr. Ing, Roberto Turri, the supervisor of Padua University, for the opportunity gives to me and for having recommended.

Dr Huw Griffiths, of Cardiff University supervisor for helping me during the field tests.

Ing. Ph.D Salah Mousa for sharing his knowledge.

Hee Jin Yang, who with great patience reminded me not to give up in hard times.

I miei familiari che hanno fatto sentire il loro amore ancora più forte di prima.

Ai miei amici che sono stati un punto di riferimento ed di non avermi mai fatto dimenticare quali sono i valori importanti.

Ing. Alice Gazzola per avermi aiutato ad inserirmi in un mondo tutto nuovo.

L'ufficio Erasmus di Padua e Cardiff per la loro grande disponibilità.



## Appendix A

### Calculation of the mutual coupling

This Appendix summarizes the formula of the a.c. mutual impedance between angled and parallel oriented conductors as reported [7].

### Mutual Coupling between parallel conductors

The figure 56 shows the orientation of the potential conductor, P, relative to the current conductor C. The voltage induced in P due to current , I, in conductor C is found by Neuman's Integral which sums the potentials induced in each incremental length "dX" of P by incremental length "dX" of C :

$$V_{md} = j \frac{\omega \mu_0 I}{4\pi} \int_0^P \int_0^P \frac{dX dX_0}{r_d}$$

where :

$$r_d = \sqrt{\left( (X - X_0) + Y_p^2 + (h_c - h_p)^2 \right)}$$

$$h_a^2 = (h_c - h_p)^2$$

P and C = length of potential conductor and current conductor respectively in m

Yp = separation between current and potential conductor

The direct mutual coupling between current and potential:

$$Md = \int_0^P \int_0^C \frac{dX dX_0}{\sqrt{\left( (X - X_0) + Y_p^2 + (h_c - h_p)^2 \right)}} = C \ln \frac{C + \sqrt{(C^2 + Y_p^2 + h_A^2)}}{C - P \sqrt{\left( (C - P)^2 + Y_p^2 + h_A^2 \right)}} + P \ln \frac{P + \sqrt{(P^2 + Y_p^2 + h_A^2)}}{P - C \sqrt{\left( (C - P)^2 + Y_p^2 + h_A^2 \right)}} + \sqrt{\left( (C - P)^2 + Y_p^2 + h_A^2 \right)} + \sqrt{(Y_p^2 + h_A^2)} - \sqrt{(C^2 + Y_p^2 + h_A^2)} - \sqrt{(P^2 + Y_p^2 + h_A^2)}$$

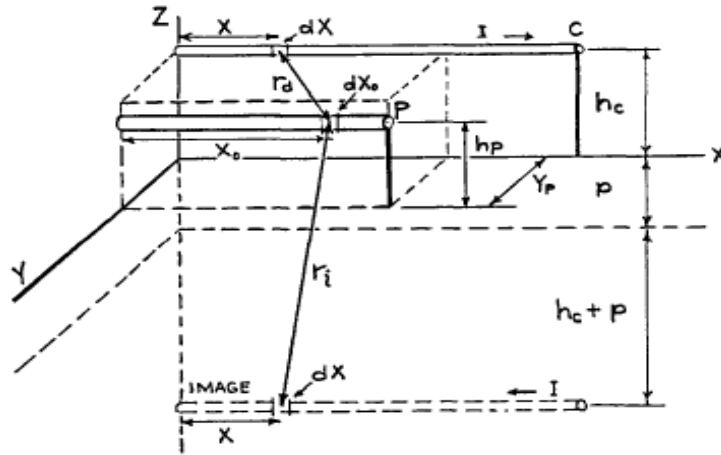


Figure 60 Mutual coupling between parallel ground return conductors

The voltage induced in P due to current I, in the image conductor C is found summing all the potentials induced in each incremental length “dX<sub>0</sub>” of P by incremental length “dX” of C :

$$V_{mi} = j \frac{\omega \mu_0 I}{4\pi} \int_0^P \int_0^C \frac{dX dX_0}{r_i}$$

Where

$$r_i = \sqrt{\left( (X - X_0)^2 + Y_p^2 + (h_c + h_p + 2p)^2 \right)}$$

The mutual coupling between image and potential conductors is :

$$M_i = \int_0^P \int_0^C \frac{dX dX_0}{\sqrt{\left( (X - X_0)^2 + Y_p^2 + (h_c + h_p + 2p)^2 \right)}} = C \ln \frac{C + \sqrt{\left( C^2 + Y_p^2 + (h_b + 2p)^2 \right)}}{C - P \sqrt{\left( (C - P)^2 + Y_p^2 + (h_b + 2p)^2 \right)}} +$$

$$P \ln \frac{P + \sqrt{\left( P^2 + Y_p^2 + (h_b + 2p)^2 \right)}}{P - C \sqrt{\left( (C - P)^2 + Y_p^2 + (h_b + 2p)^2 \right)}} +$$

$$\sqrt{\left( Y_p^2 + (h_b + 2p)^2 \right)} - \sqrt{\left( C^2 + Y_p^2 + (h_b + 2p)^2 \right)} - \sqrt{\left( P^2 + Y_p^2 + (h_b + 2p)^2 \right)}$$

where

$$h_b = h_c + h_p$$

### Mutual Coupling between angled conductors

With angled wires the calculation of mutual coupling is based on the same methods used for parallel conductors. The conductor P, as shown in the figure 61, it is divided into segments parallel to the conductor path from C to which current is calculated for each therefore rated the mutual coupling, the total mutual coupling will be the sum of the

contributions of the individual segments. More segments are used, the more accurate the result.

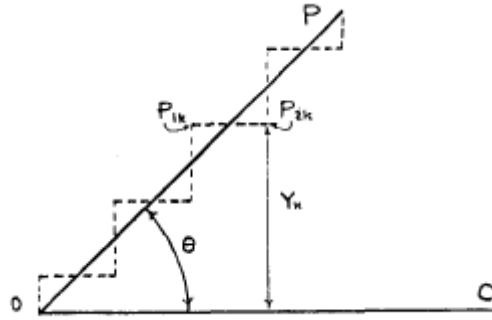


Figure 61 Modelling angled conductors with parallel segments

where:

$$P_{1k} = \frac{k-1}{n} P \cos \theta ; P_{2k} = \frac{k}{n} P \cos \theta ; Y_k = \frac{2k-1}{2n} P \sin \theta ; N = \text{number of parallel segments}$$

Direct mutual coupling between current and potential

$$M_d = \sum_{k=1}^n \left[ C \ln \frac{P_{2k}-C + \sqrt{((C-P_{2k})^2 + Y_k^2 + (h_b+2p)^2)}}{P_{1k}-C + \sqrt{((C-P_{1k})^2 + Y_k^2 + (h_b+2p)^2)}} + P_{2k} \ln \frac{P_{2k} + \sqrt{(P_{2k} + Y_k^2 + (h_b+2p)^2)}}{P_{2k}-C + \sqrt{((C-P_{2k})^2 + Y_k^2 + (h_b+2p)^2)}} - \right. \\ \left. P_{1k} \ln \frac{P_{1k} + \sqrt{(P_{1k} + Y_k^2 + (h_b+2p)^2)}}{P_{1k}-C + \sqrt{((C-P_{1k})^2 + Y_k^2 + (h_b+2p)^2)}} + \sqrt{((C-P_{2k})^2 + Y_k^2 + (h_b+2p)^2)} - \sqrt{((C-P_{1k})^2 + Y_k^2 + (h_b+2p)^2)} - \sqrt{(P_{2k}^2 + Y_k^2 + (h_b+2p)^2)} - \sqrt{(P_{1k}^2 + Y_k^2 + h_A^2)} \right]$$

The mutual coupling between image and potential conductors is :

$$M_i = \sum_{k=1}^n \left[ C \ln \frac{P_{2k}-C + \sqrt{((C-P_{2k})^2 + Y_k^2 + h_A^2)}}{P_{1k}-C + \sqrt{((C-P_{1k})^2 + Y_k^2 + h_A^2)}} + P_{2k} \ln \frac{P_{2k} + \sqrt{(P_{2k} + Y_k^2 + h_A^2)}}{P_{2k}-C + \sqrt{((C-P_{2k})^2 + Y_k^2 + h_A^2)}} - \right. \\ \left. P_{1k} \ln \frac{P_{1k} + \sqrt{(P_{1k} + Y_k^2 + h_A^2)}}{P_{1k}-C + \sqrt{((C-P_{1k})^2 + Y_k^2 + h_A^2)}} + \sqrt{((C-P_{2k})^2 + Y_k^2 + h_A^2)} - \sqrt{((C-P_{1k})^2 + Y_k^2 + (h_b+2p)^2)} - \sqrt{(P_{2k}^2 + Y_k^2 + (h_b+2p)^2)} - \sqrt{(P_{1k}^2 + Y_k^2 + (h_b+2p)^2)} \right]$$





## Appendix B

### Equipment used

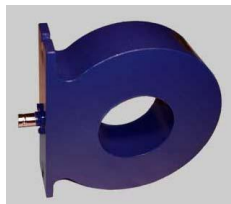
The main characteristics of the instruments was used in the different tests are summed up.

- IMS (Impedance Measurement System) is constituted essentially of two parts: EG&G Model 7260 Lock in Amplifier + QSC Audio Power Amplifier, 2400 Watts as Fig () shows. The lock-in amplifier oder instrument with dual capability. It can recover signals in the presence oder overwhelming noise background or alternatively it can provide high resolution measurements of relatively clean signals over several odersi of magnitude and frequency. Moreover it can be used as frequency and phase meter.



- Lilco wideband (0.1 V/A)

Model number	Output V/A(1)	SINEWAVE			DC saturation	Max.	Peak current
		3dB Bandwidth		Ipeak/f	current Isat A	rms Current	Ipeak A
		Lf Hz	Hf MHz	A/Hz		Irms A	
58MH100	0.10	1.5	20	2.0	2.0	100	5000



- Differential probe Chauvin Armoux DP 25

Attenuation	1/20, 1/50 and 1/200
bandwidth	0 to 25 MHz
Maximum Input Voltage	up to 1.300V peak



- Oscilloscope Lecroy wave runner 64 Xi

bandwidth	500 MHz
Channels	4
Standard Memory Length	500 kpts/ch
Max. Sample Rate	2GS/s (2 Channels)
Max. Capture Time	500 μs



- Voltage regulator Hossoni SV-4A

Capacity	1000 VA
Max. Current	4 amp
Phase	1
Input	220 V 50-60 Hz
Output	0-250 V



- Isolating transformer BBH windings LTD

Input	240 V
Output	240V
Cont. Rating	1000VA



## References

- [1] IEEE Std 80-2000 : IEEE Guide for Safety in AC Substation Grounding.
- [2] ANSI/IEEE Std 81-1983 : IEEE Guide for Measuring Earth Resistivity, Ground Impedance, and Earth Surface Potentials of a Ground System.
- [3] IEEE Std 81.2-1991 : IEEE Guide for Measurement of Impedance and Safety Characteristics of Large, Extended or Interconnected Grounding Systems.
- [4] Jinxi Ma, *Member, IEEE* and Farid P. Dawalibi, *Senior Member, IEE* “ Influence of Inductive Coupling Between Leads on Ground Impedance Measurements Using the Fall-of-Potential Method” IEEE TRANSACTIONS ON POWER DELIVERY, VOL. 16, NO. 4, OCTOBER 2001.
- [5] Haddad, A., Warne, D. , “ Advances in High Voltage Engineering ”, IEE Power & Energy, Series 40, The Institution of Electrical Engineers, 2004.
- [6] J. Nahman, Member,IEEE D. Salamon University of Belgrade, Yugoslavia “ Analytical expressions for the resistance of rodbeds and of combined grounding systems in non uniform soil “.
- [7] Eldon J. Rogers, L.S. Member, IEEE John F. White, Member, IEEE, “ Mutual coupling between finite lengths of parallel or angled horizontal earth return conductors “IEEE Transactions on Power Delivery, Vol. 4, No. 1, January 1989.
- [8] Phd Salah M. “ Investigation Of Soil Resistivity Survey at Llanrumney Site ” Cardiff 2010.
- [9] Jeff Jowett “ Measuring ground resistance –The fall of potential method ” Neta world, spring 2002.
- [10] R. Benato, A. Paolucci “ EHV AC Undergrounding Electrical Power Performance and Planning ” Springer, 2010.
- [11] H Griffiths, A Haddad, N Harid “ Characterisation of earthing system under high frequency and transient conditions ” High Voltage Group Cardiff University.
- [12] Marco Caneva, Thesis “ Studio degli accoppiamenti elettromagnetici nelle linee di trasmissione dell’energia elettrica e dei loro effetti sul campo magnetico “ Padua 2006.
- [13] Fabio Ronsivalle, Thesis “ Measurement of tower earth resistance and chain impedance of transmission lines equipped with earth wires ”.
- [14] Prof. GyörgyVarju “ Earth return, phenomena and impedance “ Budapest University of Technology & Economics.
- [15] Kandiah Arulanandan “Hydraulic and electrical flows in the clays” Department of Civil Engineering, University of California, 14 novembre 1968.

[16] ITU-T : Calculating induced voltages and currents in practical cases, Volume II., ITU, 1989 Geneva.